Composite Structures 94 (2011) 50–67

Contents lists available at ScienceDirect

Composite Structures

journal homepage: www.elsevier.com/locate/compstruct

Advanced variable kinematics Ritz and Galerkin formulations for accurate buckling and vibration analysis of anisotropic laminated composite plates

Fiorenzo Adolfo Fazzolari [a,*], Erasmo Carrera [b]

[a] School of Engineering and Mathematical Sciences, City University London, Northampton Square 0HB, London, United Kingdom
[b] Aeronautics and Space Engineering Department, Politecnico di Torino, Corso Duca degli Abruzzi 24, 10129 Torino, Italy

ARTICLE INFO

Article history:
Available online 28 July 2011

Keywords:
Advanced hierarchical plate theories
Anisotropic laminate composite plates
Approximate solution methods
Buckling
Free-vibrations

ABSTRACT

Accurate free-vibrations and linearized buckling analysis of anisotropic laminated plates with different lamination schemes and simply supported boundary condition are addressed in this paper. Approximation methods, such as Rayleigh-Ritz, Galerkin and Generalized Galerkin, based on Principle of Virtual Displacement are derived in the framework of Carrera's Unified Formulation (CUF). CUF widely used in the analysis of composite laminate beams, plates and shells, have been here formulated both for the same and different expansion orders, for the displacement components, in the thickness layer-plate direction. An extensive assessment of advanced and refined plate theories, which include Equivalent single Layer (ESL), Zig-Zag (ZZ) and Layer-wise (LW) models, with increasing number of displacement variables is provided. Accuracy of the results is shown to increase by refining the theories. Convergence studies are made in order to demonstrate that accurate results are obtained examining thin and thick plates using trigonometric approximation functions. The effects of boundary terms, upon frequency parameters and critical loads are evaluated. The effects of the various parameters (material, number of layers, fiber orientation, thickness ratio, orthotropic ratio) upon the frequencies and critical loads are discussed as well. Numerical results are compared with 3D exact solution when available from the open literature.

1. Introduction

The extreme conditions in which thin-walled aerospace structures usually work, force the design engineers to an accurate free-vibration and buckling analysis, in order to evaluate the most significant natural frequencies and critical loads of the structure. When a thin-walled structures is subject to a certain critical load the equilibrium configuration change suddenly (buckling). A simplified approach to calculate the ith critical load, is to considered the critical load as the load at which more than one infinitesimally adjacent equilibrium configuration exist and can be identified with the ith bifurcation point (Euler's method) [57]. In a linearized stability analysis the determination of the critical load leads to a linear eigenvalues problem. This method can be successfully used for plates, since the critical equilibrium configuration shows a slight geometry change when the critical load is reached. Nevertheless as explained by Leissa [36], linearized stability analysis makes sense, if and only if, the initial in-plane loading does not produce an out-of-plane deformation. Moreover there are some cases in which Euler's method fails, in particular when thin-walled structures like shells exhibit the snap-buckling phenomena. Therefore in the latter cases the most general approach, based on the solution of the complete equilibrium and stability equations [54,3], has to be used.

Coupled with buckling phenomenon, high frequency is one of the characteristic failure modes of slender structures such as plates and shells. For these reasons, research and interest in the static and dynamic behavior of composite structures, is increased rapidly.

The first accurate treatment of plates can be attributed to Germain [32] and Lagrange [35] early in the 19th century. A good historical review of the development can be referred to in the books of Soedel [56] and Timoshenko [58]. This theory is now referred to as the classical plate theory (CPT). It uses the pure bending concept of plates in the development of the equations, where normals to the middle surface remain straight and normal. It is valid for small deformation of thin plates. The inclusion of shear deformation in the fundamental equations of plates is due to Reissner [49] and Mindlin [40]. Theories that account for shear deformation are now referred to as thick plate theories or shear deformation plate theories (SDPT).

Hearmon [33] presented what could be the first study on composite plates. Among the first to work on composite plates was Smith [55]. A consistent theory for symmetrically laminated plates was presented by Reissner and Stavski [51]. There is evidence data some Russian scientists may indeed have considered the problem earlier. Ambartsumian [1] and Lekhnitskii [39] published probably

* Corresponding author. Tel.: +44 (0)2070400224; fax: +44 (0)2070408566.
E-mail address: Fiorenzo.Fazzolari.1@city.ac.uk (F.A. Fazzolari).

0263-8223/$ - see front matter © 2011 Elsevier Ltd. All rights reserved.
doi:10.1016/j.compstruct.2011.07.018

the first book in the area of composite plates and shells. Nevertheless the original contribution by Lekhniskii has been almost ignored in the subsequent literature, even though the first method able to describe the zig-zag effect and interlaminar continuous transverse stresses was provided by Lekhniskii in [38]. On the contrary the works of Ren [53,52], were taken into account. In two papers Ren has, in fact, extended Lekhnitskii's theory to orthotropic and anisotropic plates. A further pioneering analysis was presented by Yu [63] where in plane zig-zag effect and transverse shear were both fulfilled in correspondence to the two interfaces of sandwich plate. Ashton and Whitney [2] presented fundamental equations of laminated plates. Vinson and Sierakowski [60] presented analysis of composite beams, plates and shells, while Whitney [62] presented various structural analyses including free vibration of laminated anisotropic plate, and in [61] applied an extended Abartasumian theory to generally anisotropic and symmetrical and nonsymmetrical plates. The subject was also picked up by Mohan and Kingsbury [41] as well as Noor [44] among the many researchers in the field. In addition to the previous articles and books, more recent literature on composite plate vibrations research, such as Qatu [46,47], Leissa and Narita [37], can be found in various conference proceedings and journals. A complete historical review of so called zig-zag theories for laminated structures has been provided by Carrera in [15].

During the last two decades, a variable kinematics 2D models approach with hierarchical capabilities, for composite laminated plates and shells, in many papers has been widely developed by Carrera. The primary work contribution is provided in [4], where a generalization, proposing a systematic use of Reissner Mixed Variational Theorem (RMVT) [50] as a tool to furnish a class of two dimensional theories for multilayered plates analysis was presented. Attention was focused on approximated solution techniques, and the resulting governing equation were written as a system of algebraic equations. A weak form of Hooke's law was also introduced into this work to reduce the mixed cases to the displacement ones. Further details above hierarchical theories was provided in [14], where it is also available an overview of finite elements that have been developed for multilayered, anisotropic composite plates and shells, and [16] where assessment and benchmarking were performed in order to validate the 2D hierarchical models developed. Application of what is reported in [4,5] to derive governing equation in strong forms have been given in several other papers [8,7,6,10,9,12,11], where both Navier-type close form and Finite element solutions were given. Finite element formulation was also extensively developed in [19,20], where different loadings as well as boundary conditions were treated. The variable kinematics modeling technique based on Carrera's Unified Formulation (CUF) offers a systematic procedure to obtain refined structural models by considering the order of the theory as a free parameter of the formulation. In the framework of those axiomatic approaches which can be developed on the basis of variational statements, CUF attention has been restricted to Principle of Virtual Displacement (PVD) and RMVT applications (see [13]).

The accuracy of CUF has been successfully demonstrated to range from classical 2D models to quasi-3D descriptions for buckling, bending and free-vibration analyses. CUF applications have been restricted to closed form 'exact' solutions of Navier-type, and Finite element solutions. Closed form solutions are restricted to simple geometries, simply supported boundary conditions and orthotropic behavior, while FE solutions are difficult to be obtained for those case in which higher modes and/or wave propagation description is required. The use of CUF in conjunction to other approximated solution technique could be therefore of interest for a more complete description of buckling and vibration response of laminated plates. For free vibration analysis some attempts have been recently made by Ferreira who has applied Radial Basis methods [31] by CUF, and the authors [21] by applying a Ritz formulation, further application of Ritz method to CUF has been provided in [30], in which specific base functions were used to analyze plates with various in-plane forms. On that line in this paper, different approximation methods have been embedded in the framework of CUF, in order to perform buckling and free-vibration analysis of anisotropic, simply supported laminated plates. Different expansion orders for each unknown have been used. Further papers which give a guideline in order to apply the right theory depending on the problem addressed, can be find in, [24,23,22]. Only closed form solution [29], and FE applications [43] have been applied to buckling CUF formulated problems. An extensive assessment of the presented advanced and refined hierarchic ESL, ZZ and LW models both for buckling and for vibration analysis is provided. The boundary terms, which become extremely important for the accuracy of the approximate results when the angle ply lamination schemes are addressed, have been considered, and their effect upon frequency parameter and critical load discussed. By virtue of these procedures it has been possible to overcome the limits which are typical in Finite element method (FEM) as far as dynamic analysis at high frequencies is concerned. Indeed in a more general case the accuracy of FEM is very low, for a given number of degrees of freedom, because each basis function is a polynomial of low degree. On the contrary, the present methodologies use global basis functions such as trigonometric functions over the entire computational domain. When fast iterative matrix solvers are used, the present methodology can be much more efficient and accurate than FEM.

Plate geometry and notation for displacements, stresses and strains as well as Hooke's law are shown in Section 2. The variable kinematics modeling technique based on CUF is provided in Section 3. The proposed approximation method is widely described in Section 4. Governing differential equations are given in Section 5. Finally In Section 6, the results are presented. In the first part uniaxial, biaxial and pure shear in plane loads have been considered and the respective critical loads have been determined for both cross-ply and angle ply laminates. A wide assessment of the proposed variable kinematics models is carried out, and the effects of the various parameters (material, number of layers, fiber orientation, orthotropic ratio) upon the critical loads are discussed. In the second part vibration analysis of symmetric angle-ply laminates is executed, convergence analysis for the nondimensionalized frequency parameters are made in order to evaluate the influence of the plate theory and thickness ratio used. A careful discussion upon the influence of the boundary terms is provided. Finally in Section 7, the main conclusions drawn from the analysis are discussed.

2. Geometric and constitutive relations

The salient features of plate geometry are shown in Fig. 1. A laminated plate composed of N_l layers is considered. The integer k, used as superscript or subscript, denotes the layer number which starts from the bottom of the plate. The layer geometry is denoted by the same symbols as those used for the whole multilayered plate and vice versa. With x and y the plate middle surface Ω_k coordinates are indicated. Γ_k is the layer boundary on Ω_k. z and z_k are the plate and layer thickness coordinates; h and h_k denote the plate and layer thicknesses, respectively. $\zeta_k = 2z_k/h_k$ is the non-dimensioned local plate-coordinate; A_k denotes the k-layer thickness domain. Symbols that are not affected by the k subscript/superscripts refer to the whole plate. The notation for the displacement vector is:

$$\boldsymbol{u} = \{\, u_x \quad u_y \quad u_z \,\}^T \tag{1}$$

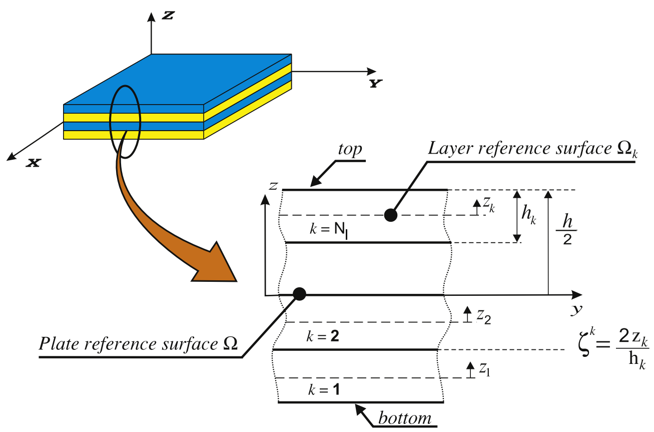

Fig. 1. Multilayered plate geometry.

Superscript T represents the transposition operator. The stresses, $\boldsymbol{\sigma}$, and the strains, $\boldsymbol{\varepsilon}$, are grouped as it follows:

$$\boldsymbol{\sigma}^k_{pH} = \left\{ \sigma^k_{xx} \quad \sigma^k_{yy} \quad \sigma^k_{xy} \right\}^T, \quad \boldsymbol{\varepsilon}^k_{pG} = \left\{ \varepsilon^k_{xx} \quad \varepsilon^k_{yy} \quad \gamma^k_{xy} \right\}^T$$
$$\boldsymbol{\sigma}^k_{nH} = \left\{ \sigma^k_{xz} \quad \sigma^k_{yz} \quad \sigma^k_{zz} \right\}^T, \quad \boldsymbol{\varepsilon}^k_{nG} = \left\{ \gamma^k_{xz} \quad \gamma^k_{yz} \quad \varepsilon^k_{zz} \right\}^T \tag{2}$$

The subscripts n and p denote transverse (out-of-plane, normal) and in-plane values,respectively, whilst the subscript H and G state that Hooke's law and geometrical relations are used. In case of small displacements with respect to in-plan dimension, the strain–displacement relations are:

$$\boldsymbol{\varepsilon}^k_{pG} = \boldsymbol{D}_p \boldsymbol{u}^k$$
$$\boldsymbol{\varepsilon}^k_{nG} = \boldsymbol{D}_n \boldsymbol{u}^k = (\boldsymbol{D}_{np} + \boldsymbol{D}_{nz}) \boldsymbol{u}^k \tag{3}$$

where $\boldsymbol{D}_p$, $\boldsymbol{D}_{np}$ and $\boldsymbol{D}_{nz}$ are differential matrix operators:

$$\boldsymbol{D}_p = \begin{bmatrix} \frac{\partial}{\partial x} & 0 & 0 \\ 0 & \frac{\partial}{\partial y} & 0 \\ \frac{\partial}{\partial y} & \frac{\partial}{\partial x} & 0 \end{bmatrix}, \quad \boldsymbol{D}_{np} = \begin{bmatrix} 0 & 0 & \frac{\partial}{\partial x} \\ 0 & 0 & \frac{\partial}{\partial y} \\ 0 & 0 & 0 \end{bmatrix}, \quad \boldsymbol{D}_{nz} = \begin{bmatrix} \frac{\partial}{\partial z} & 0 & 0 \\ 0 & \frac{\partial}{\partial z} & 0 \\ 0 & 0 & \frac{\partial}{\partial z} \end{bmatrix} \tag{4}$$

In the case of orthotropic materials, Hooke's law holds:

$$\boldsymbol{\sigma}^k = \boldsymbol{C}^k \boldsymbol{\varepsilon}^k \tag{5}$$

According to Eq. (2), the previous equation becomes:

$$\boldsymbol{\sigma}^k_{pH} = \widetilde{\boldsymbol{C}}^k_{pp} \boldsymbol{\varepsilon}_{pG} + \widetilde{\boldsymbol{C}}^k_{pn} \boldsymbol{\varepsilon}^k_{nG}$$
$$\boldsymbol{\sigma}^k_{nH} = \widetilde{\boldsymbol{C}}^k_{np} \boldsymbol{\varepsilon}_{pG} + \widetilde{\boldsymbol{C}}^k_{nn} \boldsymbol{\varepsilon}^k_{nG} \tag{6}$$

where matrices $\widetilde{\boldsymbol{C}}_{pp}$, $\widetilde{\boldsymbol{C}}_{nn}$, $\widetilde{\boldsymbol{C}}_{pn}$ and $\widetilde{\boldsymbol{C}}_{np}$ are:

$$\widetilde{\boldsymbol{C}}_{pp} = \begin{bmatrix} \widetilde{C}_{11} & \widetilde{C}_{12} & \widetilde{C}_{16} \\ \widetilde{C}_{12} & \widetilde{C}_{22} & \widetilde{C}_{26} \\ \widetilde{C}_{16} & \widetilde{C}_{26} & \widetilde{C}_{66} \end{bmatrix}, \quad \widetilde{\boldsymbol{C}}_{nn} = \begin{bmatrix} \widetilde{C}_{55} & \widetilde{C}_{45} & 0 \\ \widetilde{C}_{45} & \widetilde{C}_{44} & 0 \\ 0 & 0 & \widetilde{C}_{33} \end{bmatrix},$$
$$\widetilde{\boldsymbol{C}}_{pn} = \widetilde{\boldsymbol{C}}^T_{np} = \begin{bmatrix} 0 & 0 & \widetilde{C}_{13} \\ 0 & 0 & \widetilde{C}_{23} \\ 0 & 0 & \widetilde{C}_{36} \end{bmatrix} \tag{7}$$

For the sake of conciseness, the dependence of the coefficients $\widetilde{C}_{ij}$ versus Young's moduli, Poisson's ratio, the shear moduli and the fiber angle is not reported. It can be found in Tsai [59], Reddy [48] or Jones [34].

3. CUF for advanced and refined plates theories

In the framework of Carrera Unified Formulation (CUF) the displacement field is assumed as:

$$\boldsymbol{u} = F_\tau \boldsymbol{u}_\tau, \quad \tau = 0, 1, \ldots, N \tag{8}$$

where F_τ are functions of the coordinates z in the thickness layer-plate direction. $\boldsymbol{u}_\tau$ is the displacement vector and N stands for the number of terms of the expansion. According to Einstein's notation, the repeated subscript τ indicates summation. In this case it is possible to build hierarchical theories depending from the maximum expansion order, N. For instance, if a Equivalent single layer theory is performed and the expansion order is supposed to be 5, then using Taylor polynomials the displacement field assumes the following form:

$$\begin{aligned} u_x &= u_{x_0} + z u_{x_1} + z^2 u_{x_2} + z^3 u_{x_3} + z^4 u_{x_4} + z^5 u_{x_5} \\ u_y &= u_{y_0} + z u_{y_1} + z^2 u_{y_2} + z^3 u_{y_3} + z^4 u_{y_4} + z^5 u_{y_5} \\ u_z &= u_{z_0} + z u_{z_1} + z^2 u_{z_2} + z^3 u_{z_3} + z^4 u_{z_4} + z^5 u_{z_5} \end{aligned} \tag{9}$$

A thorough description of the refined model used can be found in [16].

Furthermore CUF can also be formulated treating each unknown independently from the others. The displacement components can be expanded with different orders, then the number of terms that can be taken into account in the expansion will depend on three different expansion indexes, N_{u_x}, N_{u_y} and N_{u_z}. The displacement field assumes the following form:

$$\begin{aligned} u_x &= F_{\tau_{u_x}} \boldsymbol{u}_{\tau_{u_x}}, \quad \tau_{u_x} = 0, 1, \ldots, N_{u_x} \\ u_y &= F_{\tau_{u_y}} \boldsymbol{u}_{\tau_{u_y}}, \quad \tau_{u_y} = 0, 1, \ldots, N_{u_y} \\ u_z &= F_{\tau_{u_z}} \boldsymbol{u}_{\tau_{u_z}}, \quad \tau_{u_z} = 0, 1, \ldots, N_{u_z} \end{aligned} \tag{10}$$

A second example is provided in order to show the difference between the two approaches. In the following case the expansion indexes are $N_{u_x} = 5$, $N_{u_y} = 1$, $N_{u_z} = 3$:

$$\begin{aligned} u_x &= u_{x_0} + z u_{x_1} + z^2 u_{x_2} + z^3 u_{x_3} + z^4 u_{x_4} + z^5 u_{x_5} \\ u_y &= u_{y_0} + z u_{y_1} \\ u_z &= u_{z_0} + z u_{z_1} + z^2 u_{z_2} + z^3 u_{z_3} \end{aligned} \tag{11}$$

a deeper description of this methodology is given in [27]. Nevertheless, the methodologies are only apparently different, indeed they can be generated using a mathematical formalism which encompasses all the possible plates theories as already proved in [4]. As already said CUF has been also used in a more general framework to include any displacement fields in [24,22]. From a computation point of view a slight difference appears in the implementation, when the expansion of the fundamental nuclei is performed, as clearly shown in [28]. By considering

$$\boldsymbol{F}_\tau = \begin{bmatrix} F_{\tau_{u_x}} & 0 & 0 \\ 0 & F_{\tau_{u_y}} & 0 \\ 0 & 0 & F_{\tau_{u_z}} \end{bmatrix}, \quad \boldsymbol{u}_\tau = \begin{bmatrix} \boldsymbol{u}_{\tau_{u_x}} & 0 & 0 \\ 0 & \boldsymbol{u}_{\tau_{u_x}} & 0 \\ 0 & 0 & \boldsymbol{u}_{\tau_{u_x}} \end{bmatrix} \tag{12}$$

in the Eq. (10), it assumes the same form of the Eq. (8):

$$\boldsymbol{u} = \boldsymbol{F}_\tau \boldsymbol{u}_\tau, \quad \tau = \tau_{u_x}, \tau_{u_y}, \tau_{u_z} \tag{13}$$

Applying this substitution all the possible *fundamental nuclei* that can be generated by using different theories and coming from the two approaches are mathematically invariant, as will be proved in Section 4.

3.1. Advanced high order shear deformation theories by using CUF

Firstly, classical models are considered. As usual, the displacement variables are expressed in Taylor series in terms of unknown variables which are defined on the plate reference surface Ω.

$$\begin{aligned} u_x &= u_{x_0} + z^{r_{u_x}} u_{r_{u_x}}, \quad r_{u_x} = 1,2,\ldots,N_{u_x} \\ u_y &= u_{y_0} + z^{r_{u_y}} u_{r_{u_y}}, \quad r_{u_y} = 1,2,\ldots,N_{u_y} \\ u_z &= u_{z_0} + z^{r_{u_z}} u_{r_{u_z}}, \quad r_{u_z} = 1,2,\ldots,N_{u_z} \end{aligned} \tag{14}$$

and in a compact unified form:

$$\boldsymbol{u} = \boldsymbol{u}_0 + z^r \boldsymbol{u}_r, \quad r = r_{u_x}, r_{u_y}, r_{u_z} \tag{15}$$

N_{u_x}, N_{u_y}, N_{u_z} are free parameters of the model. Different values for different modelings and different displacement components are assumed. The repeated r indexes are summed over their ranges. Subscript 0 denotes displacement values with correspondence to the plate reference surface Ω. Linear and higher order distributions in the z-direction are introduced by the r-polynomials (see Fig. 2). The assumed models can be written with the same notations that will be adopted for the layer-wise model Eq. (14) is therefore rewritten as

$$\begin{aligned} u_x &= F_{b_{u_x}} u_{b_{u_x}} + F_{r_{u_x}} u_{r_{u_x}} + F_{t_{u_x}} u_{t_{u_x}} = F_{\tau_{u_x}} \boldsymbol{u}_{\tau_{u_x}} \\ \tau_{u_x} &= b_{u_x}, r_{u_x}, t_{u_x} \quad r_{u_x} = 1,2,3,\ldots,N_{u_x}-1 \\ u_y &= F_{b_{u_y}} u_{t_{u_y}} + F_{r_{u_y}} u_{r_{u_y}} + F_{t_{u_y}} u_{b_{u_y}} = F_{\tau_{u_y}} \boldsymbol{u}_{\tau_{u_y}} \\ \tau_{u_y} &= b_{u_y}, r_{u_y}, t_{u_y} \quad r_{u_y} = 1,2,3,\ldots,N_{u_y}-1 \\ u_z &= F_{b_{u_z}} u_{t_{u_z}} + F_{r_{u_z}} u_{r_{u_z}} + F_{t_{u_z}} u_{b_{u_z}} = F_{\tau_{u_z}} \boldsymbol{u}_{\tau_{u_z}} \\ \tau_{u_z} &= b_{u_z}, r_{u_z}, t_{u_z} \quad r_{u_z} = 1,2,3,\ldots,N_{u_z}-1 \end{aligned} \tag{16}$$

or

$$\boldsymbol{u} = \boldsymbol{F}_\tau \boldsymbol{u}_\tau, \quad \tau = \tau_{u_x}, \tau_{u_y}, \tau_{u_z} \tag{17}$$

Subscript b denotes values related to the plate reference surface $\Omega(\boldsymbol{u}_b = \boldsymbol{u}_0)$ while subscript t refers to the highest term $(\boldsymbol{u}_t = \boldsymbol{u}_N)$. The F_τ functions assume the following explicit form:

$$\begin{aligned} F_{b_{u_x}} &= 1, \quad F_{r_{u_x}} = z^{r_{u_x}}, \quad F_{t_{u_x}} = z^{N_{u_x}}, \quad r_{u_x} = 2,3,\ldots,N_{u_x}-1 \\ F_{b_{u_y}} &= 1, \quad F_{r_{u_y}} = z^{r_{u_y}}, \quad F_{t_{u_y}} = z^{N_{u_y}}, \quad r_{u_y} = 2,3,\ldots,N_{u_y}-1 \\ F_{b_{u_z}} &= 1, \quad F_{r_{u_z}} = z^{r_{u_z}}, \quad F_{t_{u_z}} = z^{N_{u_z}}, \quad r_{u_z} = 2,3,\ldots,N_{u_z}-1 \end{aligned} \tag{18}$$

Classical models violate interlaminar equilibria of the transverse stresses. Further they do not describe zigzag form of the displacement field in plate thickness direction.

3.2. Advanced high order shear deformation theories with Murakami zig-zag effects by using CUF

The expansion given in Eq. (14) does not permit the description of the zig-zag effects. Such a limitation could somehow be overcome by referring to Murakami's idea. Murakami [42] proposed adding a zig-zag function to Eq. (14),

$$\begin{aligned} u_x &= u_{x_0} + z^{r_{u_x}} u_{r_{u_x}} + u_{Z_{u_x}} (-1)^k \zeta_k, \quad r_{u_x} = 1,2,\ldots,N_{u_x} \\ u_y &= u_{y_0} + z^{r_{u_y}} u_{r_{u_y}} + u_{Z_{u_y}} (-1)^k \zeta_k, \quad r_{u_y} = 1,2,\ldots,N_{u_y} \\ u_z &= u_{z_0} + z^{r_{u_z}} u_{r_{u_z}} + u_{Z_{u_z}} (-1)^k \zeta_k, \quad r_{u_z} = 1,2,\ldots,N_{u_z} \end{aligned} \tag{19}$$

Subscript Z refers to the introduced zig-zag term. Note that the unknown function $\boldsymbol{u}_0$, $\boldsymbol{u}_Z$, $\boldsymbol{u}_r$, are k-independent. The geometrical meaning of the zig-zag function is explained in Fig. 3. In the Murakami's function $M(z) = (-1)^k \zeta_k$ the exponent k changes the sign of the zig-zag term in each layer. Such an artifice permits one to reproduce the discontinuity of the first derivate of the displacement variables in the z-direction which physically comes from the intrinsic transverse anisotropy of multilayer structures. With unified notations Eq. (19) becomes,

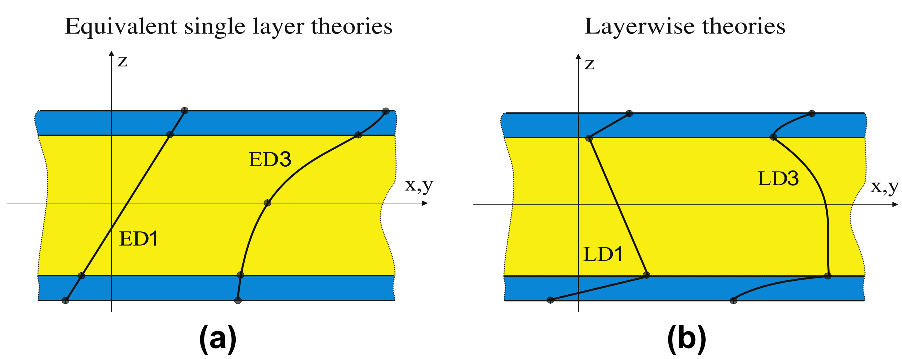

Fig. 2. ESL and LW kinematics description.

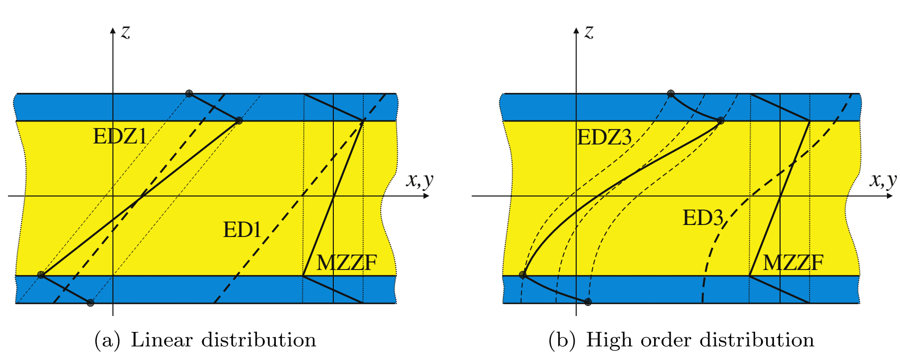

Fig. 3. Inclusion of MZZF to a linear and higher order theories.

$$
\begin{aligned}
&u_x = F_{b_{u_x}} u_{b_{u_x}} + F_{r_{u_x}} u_{r_{u_x}} + F_{t_{u_x}} u_{t_{u_x}} = F_{\tau_{u_x}} \boldsymbol{u}_{\tau_{u_x}} \\
&\tau_{u_x} = b_{u_x}, r_{u_x}, t_{u_x} \quad r_{u_x} = 1,2,3,\ldots,N_{u_x}-1 \\
&u_y = F_{b_{u_y}} u_{b_{u_y}} + F_{r_{u_y}} u_{r_{u_y}} + F_{t_{u_y}} u_{t_{u_y}} = F_{\tau_{u_y}} \boldsymbol{u}_{\tau_{u_y}} \\
&\tau_{u_y} = b_{u_x}, r_{u_y}, t_{u_y} \quad r_{u_y} = 1,2,3,\ldots,N_{u_y}-1 \\
&u_z = F_{b_{u_z}} u_{b_{u_z}} + F_{r_{u_z}} u_{r_{u_z}} + F_{t_{u_z}} u_{t_{u_z}} = F_{\tau_{u_z}} \boldsymbol{u}_{\tau_{u_z}} \\
&\tau_{u_z} = b_{u_x}, r_{u_z}, t_{u_z} \quad r_{u_z} = 1,2,3,\ldots,N_{u_z}-1
\end{aligned} \tag{20}
$$

or

$$\boldsymbol{u} = \boldsymbol{F}_\tau \boldsymbol{u}_\tau, \quad \tau = \tau_{u_x}, \tau_{u_y}, \tau_{u_z} \tag{21}$$

Subscript t refers to the introduced zig-zag term ($\boldsymbol{u}_t = \boldsymbol{u}_N$, $F_{\tau_{u_x}} = (-1)^k \zeta_k F_{\tau_{u_y}} = (-1)^k \zeta_k F_{\tau_{u_z}} = (-1)^k \zeta_k$). It should be noticed that $F_{\tau_{u_x}}, F_{\tau_{u_y}}, F_{\tau_{u_z}}$ assumes the values ±1 in correspondence to the bottom and the top interface of the k-layer (see Fig. 3). A comprehensive documentation can be found in [17,15,26].

3.3. Advanced Layerwise Theories by Using CUF

By assuming the expansion in Eq. (14) in each layer, layer-wise description is obtained. Nevertheless Taylor-type expansion of Eq. (14) is not convenient for a layer-wise description. In fact, the fulfillment of continuity requirements for the displacement at the interfaces, i.e. the C_z^0-requirement could be easily introduced by using the interface variable as unknown functions:

$$
\begin{aligned}
&u_x^k = F_{b_{u_x}} u_{b_{u_x}}^k + F_{r_{u_x}} u_{r_{u_x}}^k + F_{t_{u_z}} u_{t_{u_x}}^k = F_{\tau_{u_x}} u_{\tau_{u_x}}^k \\
&\tau_{u_x} = b_{u_x}, r_{u_x}, t_{u_x} \quad r_{u_x} = 1,2,3,\ldots,N_{u_x} \\
&u_y^k = F_{b_{u_y}} u_{b_{u_y}}^k + F_{r_{u_y}} u_{r_{u_y}}^k + F_{t_{u_y}} u_{t_{u_y}}^k = F_{\tau_{u_y}} u_{\tau_{u_y}}^k \\
&\tau_{u_y} = b_{u_y}, r_{u_y}, t_{u_y} \quad r_{u_y} = 1,2,3,\ldots,N_{u_y} \\
&u_z^k = F_{b_{u_z}} u_{b_{u_z}}^k + F_{t_{u_z}} u_{r_{u_z}}^k + F_{t_{u_z}} u_{t_{u_z}}^k = F_{\tau_{u_z}} u_{\tau_{u_z}}^k \\
&\tau_{u_z} = b_{u_z}, r_{u_z}, t_{u_z} \quad r_{u_z} = 1,2,3,\ldots,N_{u_z}
\end{aligned} \tag{22}
$$

The subscripts t and b denote values related to the layer's top and bottom surfaces, respectively. They consist of the linear part of the expansion. The thickness functions $F_\tau(\zeta_k)$ have now been defined at the k-layer level,

$$
\begin{aligned}
&F_{t_{u_x}} = \frac{P_0+P_1}{2}, \quad F_{b_{u_x}} = \frac{P_0-P_1}{2}, \quad F_{r_{u_x}} = P_{r_{u_x}} - P_{r_{u_x}-2}, \\
&r_{u_x} = 2,3,\ldots,N_{u_x} \\
&F_{t_{u_y}} = \frac{P_0+P_1}{2}, \quad F_{b_{u_y}} = \frac{P_0-P_1}{2}, \quad F_{r_{u_y}} = P_{r_{u_y}} - P_{r_{u_y}-2}, \\
&r_{u_y} = 2,3,\ldots,N_{u_y} \\
&F_{t_{u_z}} = \frac{P_0+P_1}{2}, \quad F_{b_{u_z}} = \frac{P_0-P_1}{2}, \quad F_{r_{u_z}} = P_{r_{u_z}} - P_{r_{u_z}-2}, \\
&r_{u_z} = 2,3,\ldots,N_{u_z}
\end{aligned} \tag{23}
$$

or

$$\boldsymbol{u}^k = \boldsymbol{F}_\tau \boldsymbol{u}_\tau^k, \quad \tau = \tau_{u_x}, \tau_{u_y}, \tau_{u_z} \tag{24}$$

Subscript t refers to the introduced zig-zag term in which $P_j = P_j(\zeta_k)$ is the Legendre polynomial of the j-order defined in the ζ_k-domain: $-1 \leqslant \zeta_k \leqslant 1$. Linear and cubic displacement field are shown in Fig. 2. The related polynomials are:

$$
\begin{aligned}
&P_0 = 1, \quad P_1 = \zeta_k, \quad P_2 = \frac{3\zeta_k - 1}{2} \\
&P_3 = \frac{5\zeta_k^3}{2} - \frac{3\zeta_k}{2}, \quad P_4 = \frac{35\zeta_k^4}{8} - \frac{15\zeta_k^2}{4} + \frac{3}{8}
\end{aligned} \tag{25}
$$

The chosen functions have the following properties:

$$
\zeta_k = \begin{cases} 1: F_{b_{u_x}}, F_{b_{u_y}}, F_{b_{u_z}} = 0; \quad F_{r_{u_x}}, F_{r_{u_y}}, F_{r_{u_z}} = 0; \quad F_{t_{u_x}}, F_{t_{u_y}}, F_{t_{u_z}} = 1; \\ -1: F_{b_{u_x}}, F_{b_{u_y}}, F_{b_{u_z}} = 0; \quad F_{r_{u_x}}, F_{r_{u_y}}, F_{r_{u_z}} = 0; \quad F_{t_{u_x}}, F_{t_{u_y}}, F_{t_{u_z}} = 1; \end{cases} \tag{26}
$$

The top and bottom values have been used as unknown variables. The interlaminar compatibility of displacement at each interface is easily linked:

$$\boldsymbol{u}_t^k = \boldsymbol{u}_b^{k+1}, \quad k = 1, \quad N_l - 1 \tag{27}$$

4. Approximate solution methods embedded in the framework of CUF

The coupled differential governing equations and related variationaly consistent boundary conditions, which come from the variational statement in Eq. (28), can be solved in a very few cases, that take into account particular geometries, boundary conditions and lamination schemes. Rayleigh-Ritz, Galerkin and Generalized Galerkin methods are useful methods for the approximate solutions to boundary value problems. These approaches are equally applicable to bending, buckling and vibration problems. The discrete form of the differential governing equations is obtained via the Principle of Virtual Displacements in dynamic case:

$$
\begin{aligned}
&\sum_{k=1}^{N_l} \int_{\Omega^k} \int_{A^k} \left(\delta \boldsymbol{\varepsilon}_{pG}^{k^T} \boldsymbol{\sigma}_{pH}^k + \delta \boldsymbol{\varepsilon}_{nG}^{k^T} \boldsymbol{\sigma}_{nH}^k \right) d\Omega^k \, dz \\
&\quad = \sum_{k=1}^{N_l} \int_{\Omega^k} \int_{A^k} \rho^k \delta \boldsymbol{u}^{k^T} \ddot{\boldsymbol{u}}^k \, dV + \sum_{k=1}^{N_l} \delta \boldsymbol{L}_e
\end{aligned} \tag{28}
$$

where ρ^k denotes mass density while double dots signifies accelerations. The subscript T signifies an array transposition and δ virtual variations. The variation of the internal work has been split into in-plane and out-of-plane parts and involves stresses from Hooke's law and strains from geometrical relations.

4.1. Rayleigh-Ritz method

4.1.1. Stiffness nucleus $\boldsymbol{K}$

In Rayleigh-Ritz method the displacement vector, $\boldsymbol{u}_\tau^k$, that appears in Eq. (13), and encompasses all the possible refined plate theories that can be generated by using CUF, is expressed in series expansion:

$$\boldsymbol{u}_\tau^k = \mathbf{g}_i \boldsymbol{U}_{\tau i}^k \quad \text{where} \quad i = 1,\ldots,\mathcal{N} \quad \tau = \tau_{u_x}, \tau_{u_y}, \tau_{u_z} \tag{29}$$

$\mathcal{N}$ indicate the order of expansion in the approximation. Consequently the displacement field, in compact way, assume the following form:

$$\boldsymbol{u}^k = \boldsymbol{F}_\tau \mathbf{g}_i \boldsymbol{U}_{\tau i}^k \tag{30}$$

where

$$
\boldsymbol{U}_{\tau i}^k = \begin{Bmatrix} U_{x\tau_{u_x} i}^k e^{\imath \omega_{ij} t} \\ U_{y\tau_{u_y} i}^k e^{\imath \omega_{ij} t} \\ U_{z\tau_{u_z} i}^k e^{\imath \omega_{ij} t} \end{Bmatrix}, \quad \mathbf{g}_i = \begin{bmatrix} \psi_{x_i} & 0 & 0 \\ 0 & \psi_{y_i} & 0 \\ 0 & 0 & \psi_{z_i} \end{bmatrix},
\quad
\boldsymbol{F}_\tau = \begin{bmatrix} F_{\tau_{u_x}} & 0 & 0 \\ 0 & F_{\tau_{u_y}} & 0 \\ 0 & 0 & F_{\tau_{u_z}} \end{bmatrix} \tag{31}
$$

In the coefficients $\boldsymbol{U}_{\tau i}^k$ the temporal evolution of the solution variables is required for dynamic analysis, $\imath = \sqrt{-1}$, t is the time and ω_{ij} the circular frequency. The functions ψ_{x_i}, ψ_{z_i}, ψ_{z_i} are chosen appropriately on the type of problem. The results depend strongly on the functions that will be chosen. Convergence to the exact solution is guaranteed if the basis functions are admissible functions, i.e., they satisfy the following three point:

- be continuous as required in the variational statement (i.e., should be such that it has a nonzero contribution to the virtual work statement);
- satisfy the homogeneous form of the specified geometric boundary condition;
- the set is linearly independent and complete;

Applying Rayleigh-Ritz method, it is useful rewrite the PVD as:

$$\delta \boldsymbol{L}^k_{int} - \delta \boldsymbol{L}^k_{F_{in}} - \delta \boldsymbol{L}^k_e = 0 \tag{32}$$

where $\boldsymbol{L}_{int}$ is the internal work, $\boldsymbol{L}_{F_{in}}$ is the work done from the inertial force and $\boldsymbol{L}_e$ is the work done from the external force. Being

$$\boldsymbol{\Pi}^k = \boldsymbol{L}^k_{int} - \boldsymbol{L}^k_{F_{in}} - \boldsymbol{L}^k_e \tag{33}$$

the total potential energy functional, the Eq. (32) correspond to a minimization of the functional

$$\delta \boldsymbol{\Pi}^k = 0 \tag{34}$$

The minimization is respect to the unknown coefficients of linear combination that derived to the approximation solution in Eq. (30). In particular, $\boldsymbol{\Pi}^k$ is a function of $U^k_{x\tau_{u_x}i}$, $U^k_{y\tau_{u_y}i}$, $U^k_{z\tau_{u_z}i}$ and the condition given in Eq. (34) can be written in the following form:

$$\frac{\partial \boldsymbol{\Pi}^k}{\partial U^k_{x\tau_{u_x}i}} = 0 \quad \text{with} \quad i = 1, \ldots, \mathcal{N}; \quad \tau_{u_x} = b_{u_x}, r_{u_x}, t_{u_x}$$
$$r_{u_x} = 2, 3, \ldots, N_{u_x} - 1$$
$$\frac{\partial \boldsymbol{\Pi}^k}{\partial U^k_{y\tau_{u_y}i}} = 0 \quad \text{with} \quad i = 1, \ldots, \mathcal{N}; \quad \tau_{u_y} = b_{u_y}, r_{u_y}, t_{u_y}$$
$$r_{u_y} = 2, 3, \ldots.., N_{u_y} - 1$$
$$\frac{\partial \boldsymbol{\Pi}^k}{\partial U^k_{z\tau_{u_z}i}} = 0 \quad \text{with} \quad i = 1, \ldots, \mathcal{N}; \quad \tau_{u_z} = b_{u_z}, b_{u_z}, t_{u_z}$$
$$r_{u_z} = 2, 3, \ldots.., N_{u_z} - 1$$

The discrete form of the differential governing equations can be obtained using Eq. (28). For this purpose, the strain vectors can be written by coupling Eqs. (3) and (30) as:

$$\begin{aligned} \boldsymbol{\varepsilon}^k_{pG} &= \boldsymbol{D}_p(\boldsymbol{F}_\tau \boldsymbol{g}_i)\mathbf{U}^k_{\tau i} \\ \boldsymbol{\varepsilon}^k_{nG} &= \boldsymbol{D}_{np}(\boldsymbol{F}_\tau \boldsymbol{g}_i)\mathbf{U}^k_{\tau i} + \boldsymbol{D}_{nz}(\boldsymbol{F}_\tau \boldsymbol{g}_i)\mathbf{U}^k_{\tau i} \end{aligned} \tag{36}$$

By substituting the previous expression in Eq. (28) and using Eq. (6) the internal work becomes:

$$\begin{aligned} \delta \boldsymbol{L}^k_{int} = & \int_{\Omega^k}\int_{A^k} \delta \boldsymbol{U}^{k^T}_{\tau i}[\boldsymbol{D}_p(\boldsymbol{F}_\tau \boldsymbol{g}_i)]^T \widetilde{\boldsymbol{C}}^k_{pp}\boldsymbol{D}_p(\boldsymbol{F}_s\boldsymbol{g}_j)\boldsymbol{U}^k_{sj} d\Omega^k\, dz \\ & + \int_{\Omega^k}\int_{A^k} \delta \boldsymbol{U}^{k^T}_{\tau i}[\boldsymbol{D}_p(\boldsymbol{F}_\tau \boldsymbol{g}_i)]^T \widetilde{\boldsymbol{C}}^k_{pn}\boldsymbol{D}_{np}(\boldsymbol{F}_s\boldsymbol{g}_j)\boldsymbol{U}^k_{sj} d\Omega^k\, dz \\ & + \int_{\Omega^k}\int_{A^k} \delta \boldsymbol{U}^{k^T}_{\tau i}[\boldsymbol{D}_p(\boldsymbol{F}_\tau \boldsymbol{g}_i)]^T \widetilde{\boldsymbol{C}}^k_{pn}\boldsymbol{D}_{nz}(\boldsymbol{F}_s\boldsymbol{g}_j)\boldsymbol{U}^k_{sj} d\Omega^k\, dz \\ & + \int_{\Omega^k}\int_{A^k} \delta \boldsymbol{U}^{k^T}_{\tau i}[\boldsymbol{D}_{np}(\boldsymbol{F}_\tau \boldsymbol{g}_i)]^T \widetilde{\boldsymbol{C}}^k_{np}\boldsymbol{D}_p(\boldsymbol{F}_s\boldsymbol{g}_j)\boldsymbol{U}^k_{sj} d\Omega^k\, dz \\ & + \int_{\Omega^k}\int_{A^k} \delta \boldsymbol{U}^{k^T}_{\tau i}[\boldsymbol{D}_{np}(\boldsymbol{F}_\tau \boldsymbol{g}_i)]^T \widetilde{\boldsymbol{C}}^k_{nn}\boldsymbol{D}_{np}(\boldsymbol{F}_s\boldsymbol{g}_j)\boldsymbol{U}^k_{sj} d\Omega^k\, dz \\ & + \int_{\Omega^k}\int_{A^k} \delta \boldsymbol{U}^{k^T}_{\tau i}[\boldsymbol{D}_{np}(\boldsymbol{F}_\tau \boldsymbol{g}_i)]^T \widetilde{\boldsymbol{C}}^k_{nn}\boldsymbol{D}_{nz}(\boldsymbol{F}_s\boldsymbol{g}_j)\boldsymbol{U}^k_{sj} d\Omega^k\, dz \\ & + \int_{\Omega^k}\int_{A^k} \delta \boldsymbol{U}^{k^T}_{\tau i}[\boldsymbol{D}_{nz}(\boldsymbol{F}_\tau \boldsymbol{g}_i)]^T \widetilde{\boldsymbol{C}}^k_{np}\boldsymbol{D}_p(\boldsymbol{F}_s\boldsymbol{g}_j)\boldsymbol{U}^k_{sj} d\Omega^k\, dz \\ & + \int_{\Omega^k}\int_{A^k} \delta \boldsymbol{U}^{k^T}_{\tau i}[\boldsymbol{D}_{nz}(\boldsymbol{F}_\tau \boldsymbol{g}_i)]^T \widetilde{\boldsymbol{C}}^k_{nn}\boldsymbol{D}_{np}(\boldsymbol{F}_s\boldsymbol{g}_j)\boldsymbol{U}^k_{sj} d\Omega^k\, dz \\ & + \int_{\Omega^k}\int_{A^k} \delta \boldsymbol{U}^{k^T}_{\tau i}[\boldsymbol{D}_{nz}(\boldsymbol{F}_\tau \boldsymbol{g}_i)]^T \widetilde{\boldsymbol{C}}^k_{nn}\boldsymbol{D}_{nz}(\boldsymbol{F}_s\boldsymbol{g}_j)\boldsymbol{U}^k_{sj} d\Omega^k\, dz \end{aligned} \tag{37}$$

Recalling the general expression of the virtual work:

$$\delta \boldsymbol{L}^k_{int} = \delta \boldsymbol{U}^{k^T}_{\tau i} \boldsymbol{K}^{k\tau sij} \boldsymbol{U}^k_{sj} \tag{38}$$

By comparison with Eq. (37):

$$\begin{aligned} \boldsymbol{K}^{k\tau sij} = & \int_{\Omega^k}\int_{A^k} \Big([\boldsymbol{D}_p(\boldsymbol{F}_\tau \boldsymbol{g}_i)]^T \Big[\widetilde{\boldsymbol{C}}^k_{pp}\boldsymbol{D}_p(\boldsymbol{F}_s\boldsymbol{g}_j) + \widetilde{\boldsymbol{C}}^k_{pn}\boldsymbol{D}_{np}(\boldsymbol{F}_s\boldsymbol{g}_j) \\ & + \widetilde{\boldsymbol{C}}^k_{pn}\boldsymbol{D}_{nz}(\boldsymbol{F}_s\boldsymbol{g}_j)\Big] + [\boldsymbol{D}_{np}(\boldsymbol{F}_\tau \boldsymbol{g}_i)]^T \Big[\widetilde{\boldsymbol{C}}^k_{np}\boldsymbol{D}_p(\boldsymbol{F}_s\boldsymbol{g}_j) + \widetilde{\boldsymbol{C}}^k_{nn}\boldsymbol{D}_{np}(\boldsymbol{F}_s\boldsymbol{g}_j) \\ & + \widetilde{\boldsymbol{C}}^k_{nn}\boldsymbol{D}_{nz}(\boldsymbol{F}_s\boldsymbol{g}_j)\Big] + [\boldsymbol{D}_{nz}(\boldsymbol{F}_\tau \boldsymbol{g}_i)]^T \Big[\widetilde{\boldsymbol{C}}^k_{np}\boldsymbol{D}_p(\boldsymbol{F}_s\boldsymbol{g}_j) + \widetilde{\boldsymbol{C}}^k_{nn}\boldsymbol{D}_{np}(\boldsymbol{F}_s\boldsymbol{g}_j) \\ & + \widetilde{\boldsymbol{C}}^k_{nn}\boldsymbol{D}_{nz}(\boldsymbol{F}_s\boldsymbol{g}_j)\Big]\Big) d\Omega^k\, dz \end{aligned} \tag{39}$$

The Eq. (39) can be written in a more compact form:

$$\begin{aligned} \boldsymbol{K}^{k\tau sij} = & \sum_q \int_{\Omega^k}\int_{A^k} \Big([\boldsymbol{D}_q(\boldsymbol{F}_\tau \boldsymbol{g}_i)]^T \Big[\widetilde{\boldsymbol{C}}^k_{qp}\boldsymbol{D}_p(\boldsymbol{F}_\tau \boldsymbol{g}_i) + \widetilde{\boldsymbol{C}}^k_{qn}(\boldsymbol{D}_{np}(\boldsymbol{F}_\tau \boldsymbol{g}_i) \\ & + \boldsymbol{D}_{nz}(\boldsymbol{F}_\tau \boldsymbol{g}_i))\Big]\Big) d\Omega^k\, dz \end{aligned} \tag{40}$$

where $q = p$, n.

The stiffness matrix determined represents the *main fundamental nucleus* related to Principle of Virtual Displacements in *static* case. The Eq. (40) leads to a matrix composed of nine *secondary invariant fundamental nuclei*, for the sake of accuracy they are listed following:

$$\begin{aligned} K^{\tau_{u_x}s_{u_x}}_{u_x u_x} = & \widetilde{\boldsymbol{C}}^k_{11}\left[\int_{A^k}(F_{\tau_{u_x}}F_{s_{u_x}})dz\right]\left[\int_{\Omega^k}(\psi_{x_i,x}\psi_{x_j,x})d\Omega^k\right] \\ & + \widetilde{\boldsymbol{C}}^k_{16}\left[\int_{A^k}(F_{\tau_{u_x}}F_{s_{u_x}})dz\right]\left[\int_{\Omega^k}(\psi_{x_i,x}\psi_{x_j,y})d\Omega^k\right] \\ & + \widetilde{\boldsymbol{C}}^k_{16}\left[\int_{A^k}(F_{\tau_{u_x}}F_{s_{u_x}})dz\right]\left[\int_{\Omega^k}(\psi_{x_i,y}\psi_{x_j,x})d\Omega^k\right] \\ & + \widetilde{\boldsymbol{C}}^k_{66}\left[\int_{A^k}(F_{\tau_{u_x}}F_{s_{u_x}})dz\right]\left[\int_{\Omega^k}(\psi_{x_i,y}\psi_{x_j,y})d\Omega^k\right] \\ & + \widetilde{\boldsymbol{C}}^k_{55}\left[\int_{A^k}(F_{\tau_{u_x,z}}F_{s_{u_x,z}})dz\right]\left[\int_{\Omega^k}(\psi_{x_i}\psi_{x_j})d\Omega^k\right] \end{aligned}$$

$$\begin{aligned} K^{\tau_{u_x}s_{u_y}}_{u_x u_y} = & \widetilde{\boldsymbol{C}}^k_{16}\left[\int_{A^k}(F_{\tau_{u_x}}F_{s_{u_y}})dz\right]\left[\int_{\Omega^k}(\psi_{x_i,x}\psi_{y_j,x})d\Omega^k\right] \\ & + \widetilde{\boldsymbol{C}}^k_{12}\left[\int_{A^k}(F_{\tau_{u_x}}F_{s_{u_y}})dz\right]\left[\int_{\Omega^k}(\psi_{x_i,x}\psi_{y_j,y})d\Omega^k\right] \\ & + \widetilde{\boldsymbol{C}}^k_{66}\left[\int_{A^k}(F_{\tau_{u_x}}F_{s_{u_y}})dz\right]\left[\int_{\Omega^k}(\psi_{x_i,y}\psi_{y_j,x})d\Omega^k\right] \\ & + \widetilde{\boldsymbol{C}}^k_{26}\left[\int_{A^k}(F_{\tau_{u_x}}F_{s_{u_y}})dz\right]\left[\int_{\Omega^k}(\psi_{x_i,y}\psi_{y_j,y})d\Omega^k\right] \\ & + \widetilde{\boldsymbol{C}}^k_{45}\left[\int_{A^k}(F_{\tau_{u_x,z}}F_{s_{u_y,z}})dz\right]\left[\int_{\Omega^k}(\psi_{x_i}\psi_{y_j})d\Omega^k\right] \end{aligned}$$

$$\begin{aligned} K^{\tau_{u_x}s_{u_z}}_{u_x u_z} = & \widetilde{\boldsymbol{C}}^k_{55}\left[\int_{A^k}(F_{\tau_{u_x,z}}F_{s_{u_z}})dz\right]\left[\int_{\Omega^k}(\psi_{x_i}\psi_{z_j,x})d\Omega^k\right] \\ & + \widetilde{\boldsymbol{C}}^k_{45}\left[\int_{A^k}(F_{\tau_{u_x,z}}F_{s_{u_z}})dz\right]\left[\int_{\Omega^k}(\psi_{x_i}\psi_{z_j,y})d\Omega^k\right] \\ & + \widetilde{\boldsymbol{C}}^k_{13}\left[\int_{A^k}(F_{\tau_{u_x}}F_{s_{u_z,z}})dz\right]\left[\int_{\Omega^k}(\psi_{x_i,x}\psi_{z_j})d\Omega^k\right] \\ & + \widetilde{\boldsymbol{C}}^k_{36}\left[\int_{A^k}(F_{\tau_{u_x}}F_{s_{u_z,z}})dz\right]\left[\int_{\Omega^k}(\psi_{x_i,y}\psi_{z_j})d\Omega^k\right] \end{aligned}$$

$$\begin{aligned} K^{\tau_{u_y}s_{u_x}}_{u_y u_x} = & \widetilde{\boldsymbol{C}}^k_{16}\left[\int_{A^k}(F_{\tau_{u_y}}F_{s_{u_x}})dz\right]\left[\int_{\Omega^k}(\psi_{x_i}\psi_{y_j,xx})d\Omega^k\right] \\ & + \widetilde{\boldsymbol{C}}^k_{12}\left[\int_{A^k}(F_{\tau_{u_y}}F_{s_{u_x}})dz\right]\left[\int_{\Omega^k}(\psi_{x_i}\psi_{y_j,xy})d\Omega^k\right] \\ & + \widetilde{\boldsymbol{C}}^k_{66}\left[\int_{A^k}(F_{\tau_{u_y}}F_{s_{u_x}})dz\right]\left[\int_{\Omega^k}(\psi_{x_i}\psi_{y_j,yx})d\Omega^k\right] \\ & + \widetilde{\boldsymbol{C}}^k_{26}\left[\int_{A^k}(F_{\tau_{u_y}}F_{s_{u_x}})dz\right]\left[\int_{\Omega^k}(\psi_{x_i}\psi_{y_j,yy})d\Omega^k\right] \\ & + \widetilde{\boldsymbol{C}}^k_{45}\left[\int_{A^k}(F_{\tau_{u_y,z}}F_{s_{u_x,z}})dz\right]\left[\int_{\Omega^k}(\psi_{x_i}\psi_{y_j})d\Omega^k\right] \end{aligned}$$

$$
\begin{aligned}
K^{\tau_{u_y}s_{u_y}}_{u_yu_y} &= \widetilde{C}^k_{26}\left[\int_{A^k}(F_{\tau_{u_y}}F_{s_{u_y}})dz\right]\left[\int_{\Omega^k}(\psi_{y_i,y}\psi_{y_j,x})d\Omega^k\right] \\
&+ \widetilde{C}^k_{22}\left[\int_{A^k}(F_{\tau_{u_y}}F_{s_{u_y}})dz\right]\left[\int_{\Omega^k}(\psi_{y_i,y}\psi_{y_j,y})d\Omega^k\right] \\
&+ \widetilde{C}^k_{66}\left[\int_{A^k}(F_{\tau_{u_y}}F_{s_{u_y}})dz\right]\left[\int_{\Omega^k}(\psi_{y_i,y}\psi_{y_j,x})d\Omega^k\right] \\
&+ \widetilde{C}^k_{26}\left[\int_{A^k}(F_{\tau_{u_y}}F_{s_{u_y}})dz\right]\left[\int_{\Omega^k}(\psi_{y_i,y}\psi_{y_j,y})d\Omega^k\right] \\
&+ \widetilde{C}^k_{44}\left[\int_{A^k}(F_{\tau_{u_y},z}F_{s_{u_y},z})dz\right]\left[\int_{\Omega^k}(\psi_{y_i}\psi_{y_j})d\Omega^k\right] \\
K^{\tau_{u_y}s_{u_z}}_{u_yu_z} &= \widetilde{C}^k_{45}\left[\int_{A^k}(F_{\tau_{u_y},z}F_{s_{u_z}})dz\right]\left[\int_{\Omega^k}(\psi_{y_i}\psi_{z_j,x})d\Omega^k\right] \\
&+ \widetilde{C}^k_{44}\left[\int_{A^k}(F_{\tau_{u_y},z}F_{s_{u_z}})dz\right]\left[\int_{\Omega^k}(\psi_{y_i}\psi_{z_j,y})d\Omega^k\right] \\
&+ \widetilde{C}^k_{36}\left[\int_{A^k}(F_{\tau_{u_y}}F_{s_{u_z},z})dz\right]\left[\int_{\Omega^k}(\psi_{y_i,x}\psi_{z_j})d\Omega^k\right] \\
&+ \widetilde{C}^k_{23}\left[\int_{A^k}(F_{\tau_{u_y}}F_{s_{u_z},z})dz\right]\left[\int_{\Omega^k}(\psi_{y_i,y}\psi_{z_j})d\Omega^k\right] \\
K^{\tau_{u_z}s_{u_x}}_{u_zu_x} &= \widetilde{C}^k_{55}\left[\int_{A^k}(F_{\tau_{u_z}}F_{s_{u_x},z})dz\right]\left[\int_{\Omega^k}(\psi_{x_i}\psi_{z_j,x})d\Omega^k\right] \\
&+ \widetilde{C}^k_{45}\left[\int_{A^k}(F_{\tau_{u_z}}F_{s_{u_x},z})dz\right]\left[\int_{\Omega^k}(\psi_{x_i}\psi_{z_j,y})d\Omega^k\right] \\
&+ \widetilde{C}^k_{13}\left[\int_{A^k}(F_{\tau_{u_z},z}F_{s_{u_x}})dz\right]\left[\int_{\Omega^k}(\psi_{x_i,x}\psi_{z_j})d\Omega^k\right] \\
&+ \widetilde{C}^k_{36}\left[\int_{A^k}(F_{\tau_{u_z},z}F_{s_{u_x}})dz\right]\left[\int_{\Omega^k}(\psi_{x_i,y}\psi_{z_j})d\Omega^k\right] \\
K^{\tau_{u_z}s_{u_y}}_{u_zu_y} &= \widetilde{C}^k_{45}\left[\int_{A^k}(F_{\tau_{u_z}}F_{s_{u_y},z})dz\right]\left[\int_{\Omega^k}(\psi_{y_i}\psi_{z_j,x})d\Omega^k\right] \\
&+ \widetilde{C}^k_{44}\left[\int_{A^k}(F_{\tau_{u_z}}F_{s_{u_y},z})dz\right]\left[\int_{\Omega^k}(\psi_{y_i}\psi_{z_j,y})d\Omega^k\right] \\
&+ \widetilde{C}^k_{36}\left[\int_{A^k}(F_{\tau_{u_z},z}F_{s_{u_y}})dz\right]\left[\int_{\Omega^k}(\psi_{y_i,x}\psi_{z_j})d\Omega^k\right] \\
&+ \widetilde{C}^k_{23}\left[\int_{A^k}(F_{\tau_{u_z},z}F_{s_{u_y}})dz\right]\left[\int_{\Omega^k}(\psi_{y_i,y}\psi_{z_j})d\Omega^k\right] \\
K^{\tau_{u_z}s_{u_z}}_{u_zu_z} &= \widetilde{C}^k_{45}\left[\int_{A^k}(F_{\tau_{u_z}}F_{s_{u_z}})dz\right]\left[\int_{\Omega^k}(\psi_{z_i,y}\psi_{z_j,x})d\Omega^k\right] \\
&+ \widetilde{C}^k_{44}\left[\int_{A^k}(F_{\tau_{u_z}}F_{s_{u_z}})dz\right]\left[\int_{\Omega^k}(\psi_{z_i,y}\psi_{z_j,y})d\Omega^k\right] \\
&+ \widetilde{C}^k_{55}\left[\int_{A^k}(F_{\tau_{u_z}}F_{s_{u_z}})dz\right]\left[\int_{\Omega^k}(\psi_{z_i,x}\psi_{z_j,x})d\Omega^k\right] \\
&+ \widetilde{C}^k_{45}\left[\int_{A^k}(F_{\tau_{u_z}}F_{s_{u_z}})dz\right]\left[\int_{\Omega^k}(\psi_{z_i,x}\psi_{z_j,y})d\Omega^k\right] \\
&+ \widetilde{C}^k_{33}\left[\int_{A^k}(F_{\tau_{u_z},z}F_{s_{u_z},z})dz\right]\left[\int_{\Omega^k}(\psi_{z_i}\psi_{z_j})d\Omega^k\right]
\end{aligned}
\tag{41}
$$

Each *nucleus* or *kernel* of CUF, has to be expanded individually according to the expansion order chosen for the displacement components. When the expansions have been performed then the 9 secondary invariant nuclei arranged as in Eq. (42) generate the main fundamental nucleus related at the particular theory used. The secondary nuclei are then formally invariant both with respect to the order used for the expansion for each displacement components and with respect to the type of theory used.

$$
\boldsymbol{K}^{k\tau sij} = \begin{bmatrix} \boldsymbol{K}_{u_xu_x} & \boldsymbol{K}_{u_xu_y} & \boldsymbol{K}_{u_xu_z} \\ \boldsymbol{K}^T_{u_xu_y} & \boldsymbol{K}_{u_yu_y} & \boldsymbol{K}_{u_yu_z} \\ \boldsymbol{K}^T_{u_xu_z} & \boldsymbol{K}^T_{u_yu_z} & \boldsymbol{K}_{u_zu_z} \end{bmatrix} \tag{42}
$$

4.1.2. Mass nucleus $\boldsymbol{M}$

From the work done by the inertial force:

$$
\delta \boldsymbol{L}^k_{F_{in}} = \int_{\Omega^k}\int_{A^k} \rho^k \delta \boldsymbol{u}^{k^T} \ddot{\boldsymbol{u}}^k \, d\Omega^k \, dz \tag{43}
$$

using Eq. (30):

$$
\delta \boldsymbol{L}^k_{F_{in}} = \int_{\Omega^k}\int_{A^k} (\rho^k \delta \boldsymbol{U}^{k^T}_{\tau i}\left[(\boldsymbol{F}_\tau \boldsymbol{g}_i)^T(\boldsymbol{F}_s \boldsymbol{g}_j)\right]\ddot{\boldsymbol{U}}_{sj}) d\Omega^k \, dz \tag{44}
$$

Since

$$
\delta \boldsymbol{L}^k_{F_{in}} = \delta \boldsymbol{U}^{k^T}_{\tau i} \mathbf{M}^{k\tau sij} \ddot{\boldsymbol{U}}^k_{sj} \tag{45}
$$

comparing the two relations:

$$
\boldsymbol{M}^{k\tau sij} = \int_{\Omega^k}\int_{A^k} (\rho^k \left[(\boldsymbol{F}_\tau \boldsymbol{g}_i)^T(\boldsymbol{F}_s \boldsymbol{g}_j)\right]) d\Omega^k \, dz \tag{46}
$$

The Eq. (46) leads to a matrix composed by the three *secondary invariant fundamental nuclei*, which takes the following form:

$$
\begin{aligned}
M^{\tau_{u_x}s_{u_x}}_{u_xu_x} &= \rho^k\left[\int_{A^k} F_{\tau_{u_x}}F_{s_{u_x}}\,dz\right]\left[\int_{\Omega^k}(\psi_{x_i}\psi_{x_j})d\Omega\right] \\
M^{\tau_{u_y}s_{u_y}}_{u_yu_y} &= \rho^k\left[\int_{A^k} F_{\tau_{u_y}}F_{s_{u_y}}\,dz\right]\left[\int_{\Omega^k}(\psi_{y_i}\psi_{y_j})d\Omega\right] \\
M^{\tau_{u_z}s_{u_z}}_{u_zu_z} &= \rho^k\left[\int_{A^k} F_{\tau_{u_z}}F_{s_{u_z}}\,dz\right]\left[\int_{\Omega^k}(\psi_{z_i}\psi_{z_j})d\Omega\right]
\end{aligned}
\tag{47}
$$

and after the matrices have been expanded, the main nucleus becomes:

$$
\boldsymbol{M}^{k\tau sij} = \begin{bmatrix} \boldsymbol{M}_{u_xu_x} & 0 & 0 \\ 0 & \boldsymbol{M}_{u_yu_y} & 0 \\ 0 & 0 & \boldsymbol{M}_{u_zu_z} \end{bmatrix} \tag{48}
$$

The discrete form of the governing equations is finally obtained in terms of fundamental nuclei:

$$
\delta \boldsymbol{U}^{k^T}_{\tau i} : \boldsymbol{K}^{k\tau sij}\boldsymbol{U}^k_{sj} + \boldsymbol{M}^{k\tau sij}\ddot{\boldsymbol{U}}^k_{sj} = 0 \tag{49}
$$

The free-vibration response leads to the following *eigenvalues problem*

$$
\|\boldsymbol{K}^{k\tau sij} - \lambda_{ij}\boldsymbol{M}^{k\tau sij}\| = 0 \tag{50}
$$

where $\lambda_{ij} = \omega^2_{ij}$ are the eigenvalues of the problem, the double bar denote the determinant. This procedure has been computed for different advanced theories, as clearly shown in Section 6.

4.1.3. Initial stress nucleus $\boldsymbol{K}_\sigma$

The buckling analysis is addressed via Euler's method of adjacent equilibrium states [38]. It consists in a linearized stability analysis of an undeformed equilibrium configuration, whose critical condition is defined by a proportionally scaled load in combination with a *geometric* or *initial stress* stiffness built up from the exact nonlinear strain–displacement relations or von Kàrmàn's approximation. The linearized buckling analysis require the fulfillment of the following condition:

- The pre-buckling deformation can be neglected.
- The initial stress σ_0 remains constant and varies neither in magnitude nor in direction during buckling.
- At bifurcation the equilibrium states are infinitesimally adjacent so that a linearization is possible.

The initial stress matrix is constructed from the work done by the virtual non-linear strains with the actual initial stresses

$$\boldsymbol{\varepsilon}^k_{p_{nl}} = \left[\varepsilon^k_{xx_{nl}}, \varepsilon^k_{yy_{nl}}, \gamma^k_{xy_{nl}}\right]^T \quad \boldsymbol{\sigma}^k_{p_0} = \left[\sigma^k_{xx_0}, \sigma^k_{yy_0}, \sigma^k_{xy_0}\right]^T \tag{51}$$

$$\delta \boldsymbol{L}^k_e = \int_{\Omega^k}\int_{A^k}\left(\delta\varepsilon^k_{xx_{nl}}\sigma^k_{xx_0} + \delta\varepsilon^k_{yy_{nl}}\sigma^k_{yy_0} + \delta\gamma^k_{xy_{nl}}\sigma^k_{xy_0}\right) d\Omega^k\, dz \tag{52}$$

The buckling load can be then defined via a scalar load factor λ as the load $\sigma = \lambda\sigma_0$ for which an equilibrium configuration exists such that

$$\delta \boldsymbol{U}^{k^T}_{\tau i} : \left[\boldsymbol{K}^{k\tau sij} + \lambda_{ij}\boldsymbol{K}^{k\tau sij}_\sigma\right]\boldsymbol{U}^k_{sj} = 0 \tag{53}$$

$\boldsymbol{K}^{k\tau sij}$ is the usual linear stiffness matrix and $\boldsymbol{K}^{k\tau sij}_\sigma$ is the initial stress matrix and assumes the following form when Ritz method is performed:

$$\begin{aligned}
K^{\tau_{u_x}s_{u_x}}_{\sigma_{u_x u_x}} &= \delta_{vK}\Bigg(\sigma^k_{xx_0}\left[\int_{A^k} F_{\tau_{u_x}} F_{s_{u_x}}\, dz\right]\left[\int_{\Omega^k}(\psi_{x_i,x}\psi_{x_j,x})d\Omega\right] \\
&\quad + \sigma^k_{yy_0}\left[\int_{A^k} F_{\tau_{u_x}} F_{s_{u_x}}\, dz\right]\left[\int_{\Omega^k}(\psi_{x_i,y}\psi_{x_j,y})d\Omega\right] \\
&\quad + \sigma^k_{xy_0}\left[\int_{A^k} F_{\tau_{u_x}} F_{s_{u_x}}\, dz\right]\Bigg\{\left[\int_{\Omega^k}(\psi_{x_i,x}\psi_{x_j,y})d\Omega\right] \\
&\quad + \left[\int_{\Omega^k}(\psi_{x_i,y}\psi_{x_j,z})d\Omega\right]\Bigg\}\Bigg) \\
K^{\tau_{u_y}s_{u_y}}_{\sigma_{u_y u_y}} &= \delta_{vK}\Bigg(\sigma^k_{xx_0}\left[\int_{A^k} F_{\tau_{u_y}} F_{s_{u_y}}\, dz\right]\left[\int_{\Omega^k}(\psi_{y_i,x}\psi_{y_j,x})d\Omega\right] \\
&\quad + \sigma^k_{yy_0}\left[\int_{A^k} F_{\tau_{u_y}} F_{s_{u_y}}\, dz\right]\left[\int_{\Omega^k}(\psi_{y_i,y}\psi_{y_j,y})d\Omega\right] \\
&\quad + \sigma^k_{xy_0}\left[\int_{A^k} F_{\tau_{u_y}} F_{s_{u_y}}\, dz\right]\Bigg\{\left[\int_{\Omega^k}(\psi_{y_i,x}\psi_{y_j,y})d\Omega\right] \\
&\quad + \left[\int_{\Omega^k}(\psi_{y_i,y}\psi_{y_j,z})d\Omega\right]\Bigg\}\Bigg) \\
K^{\tau_{u_z}s_{u_z}}_{\sigma_{u_z u_z}} &= \Bigg(\sigma^k_{xx_0}\left[\int_{A^k} F_{\tau_{u_z}} F_{s_{u_z}}\, dz\right]\left[\int_{\Omega^k}(\psi_{z_i,x}\psi_{z_j,x})d\Omega\right] \\
&\quad + \sigma^k_{yy_0}\left[\int_{A^k} F_{\tau_{u_z}} F_{s_{u_z}}\, dz\right]\left[\int_{\Omega^k}(\psi_{z_i,y}\psi_{z_j,y})d\Omega\right] \\
&\quad + \sigma^k_{xy_0}\left[\int_{A^k} F_{\tau_{u_z}} F_{s_{u_z}}\, dz\right]\Bigg\{\left[\int_{\Omega^k}(\psi_{z_i,x}\psi_{z_j,y})d\Omega\right] \\
&\quad + \left[\int_{\Omega^k}(\psi_{z_i,y}\psi_{z_j,z})d\Omega\right]\Bigg\}\Bigg)
\end{aligned} \tag{54}$$

or

$$\begin{aligned}
K^{\tau_{u_x}s_{u_x}}_{\sigma_{u_x u_x}} &= \delta_{vK}\Bigg(\sigma^k_{xx_0}\left[\int_{A^k} F_{\tau_{u_x}} F_{s_{u_x}}\, dz\right]\left[\int_{\Omega^k}(\psi_{x_i,x}\psi_{x_j,x})d\Omega\right] \\
&\quad + \sigma^k_{yy_0}\left[\int_{A^k} F_{\tau_{u_x}} F_{s_{u_x}}\, dz\right]\left[\int_{\Omega^k}(\psi_{x_i,y}\psi_{x_j,y})d\Omega\right] \\
&\quad + 2\sigma^k_{xy_0}\left[\int_{A^k} F_{\tau_{u_x}} F_{s_{u_x}}\, dz\right]\left[\int_{\Omega^k}(\psi_{x_i,x}\psi_{x_j,y})d\Omega\right]\Bigg) \\
K^{\tau_{u_y}s_{u_y}}_{\sigma_{u_y u_y}} &= \delta_{vK}\Bigg(\sigma^k_{xx_0}\left[\int_{A^k} F_{\tau_{u_y}} F_{s_{u_y}}\, dz\right]\left[\int_{\Omega^k}(\psi_{y_i,x}\psi_{y_j,x})d\Omega\right] \\
&\quad + \sigma^k_{yy_0}\left[\int_{A^k} F_{\tau_{u_y}} F_{s_{u_y}}\, dz\right]\left[\int_{\Omega^k}(\psi_{y_i,y}\psi_{y_j,y})d\Omega\right] \\
&\quad + 2\sigma^k_{xy_0}\left[\int_{A^k} F_{\tau_{u_y}} F_{s_{u_y}}\, dz\right]\left[\int_{\Omega^k}(\psi_{y_i,x}\psi_{y_j,y})d\Omega\right]\Bigg) \\
K^{\tau_{u_z}s_{u_z}}_{\sigma_{u_z u_z}} &= \Bigg(\sigma^k_{xx_0}\left[\int_{A^k} F_{\tau_{u_z}} F_{s_{u_z}}\, dz\right]\left[\int_{\Omega^k}(\psi_{z_i,x}\psi_{z_j,x})d\Omega\right] \\
&\quad + \sigma^k_{yy_0}\left[\int_{A^k} F_{\tau_{u_z}} F_{s_{u_z}}\, dz\right]\left[\int_{\Omega^k}(\psi_{z_i,y}\psi_{z_j,y})d\Omega\right] \\
&\quad + 2\sigma^k_{xy_0}\left[\int_{A^k} F_{\tau_{u_z}} F_{s_{u_z}}\, dz\right]\left[\int_{\Omega^k}(\psi_{z_i,x}\psi_{z_j,y})d\Omega\right]\Bigg)
\end{aligned} \tag{55}$$

when the Galerkin or Generalized Galerkin are used. Furthermore in both cases, the tracer δ_{vK} is used to introduce von Kàrmàn's approximation. The initial stress matrix nucleus after the matrix expansion is:

$$\boldsymbol{K}^{k\tau sij}_\sigma = \begin{bmatrix} \boldsymbol{K}_{\sigma_{u_x u_x}} & 0 & 0 \\ 0 & \boldsymbol{K}_{\sigma_{u_x u_x}} & 0 \\ 0 & 0 & \boldsymbol{K}_{\sigma_{u_z u_z}} \end{bmatrix} \tag{56}$$

Then the calculus of the critical loads is similar to the free-vibration analysis, leading to an *eigenvalues problem*:

$$\|\boldsymbol{K}^{k\tau sij} + \lambda_{ij}\boldsymbol{K}^{k\tau sij}_\sigma\| = 0 \tag{57}$$

4.2. Galerkin and Generalized Galerkin methods

4.2.1. Stiffness and boundary nuclei

In this section Galerkin and Generalized Galerkin method are developed. The displacement approach is formulated by variationally imposing the equilibrium via the principle of virtual displacements. Then, PDV statement is used to derive strong form of governing differential equations and related boundary conditions. Gauss theorem should be used to move the derivatives from virtual variation. The following array formula for the integration by parts is introduced to the purpose:

$$\begin{aligned}
\int_{\Omega^k}\left[(\boldsymbol{D}_\Omega)\delta\boldsymbol{\phi}^k\right]^T\boldsymbol{\varphi}^k d\Omega^k = &-\int_{\Omega^k}\delta\boldsymbol{\phi}^{k^T}\left[(\boldsymbol{D}_\Omega)^T\boldsymbol{\varphi}\right]d\Omega^k \\
&+\int_{\Gamma^k}\delta\boldsymbol{\phi}^{k^T}\left[(\mathbf{I}_\Omega)^T\boldsymbol{\varphi}^k\right]d\Gamma^k
\end{aligned} \tag{58}$$

For sake of simplicity, it is intended that the boundary Γ^k is parallel to the direction x, y and $\boldsymbol{\phi}$ and $\boldsymbol{\varphi}$ are two generic column of displacements and stresses. $\boldsymbol{D}_\Omega$ denotes a generic array including only first order partial differential operators with respect to the in-plane coordinates x, y, and $\Omega = p, np, nz$. The array $(\mathbf{I}_\Omega)^T$ is build as follow: the unit number 1 is set with correspondence to those element of $\boldsymbol{D}_\Omega$ which are different by zero. Then the application of the Eq. (58) at the functional in Eq. (37), leads to:

$$\begin{aligned}
\delta\boldsymbol{L}^k_{int} = &-\int_{\Omega^k}\int_{A^k}\delta\boldsymbol{U}^{k^T}_{\tau i}(\boldsymbol{F}_\tau\boldsymbol{g}_i)^T\left\{(\boldsymbol{D}_p)^T\left[\widetilde{\boldsymbol{C}}^k_{pp}\boldsymbol{D}_p(\boldsymbol{F}_s\boldsymbol{g}_j)\right]\right\}\boldsymbol{U}^k_{sj}d\Omega^k dz \\
&-\int_{\Omega^k}\int_{A^k}\delta\boldsymbol{U}^{k^T}_{\tau i}(\boldsymbol{F}_\tau\boldsymbol{g}_i)^T\left\{(\boldsymbol{D}_p)^T\left[\widetilde{\boldsymbol{C}}^k_{pn}\boldsymbol{D}_{np}(\boldsymbol{F}_s\boldsymbol{g}_j)\right]\right\}\boldsymbol{U}^k_{sj}d\Omega^k dz \\
&-\int_{\Omega^k}\int_{A^k}\delta\boldsymbol{U}^{k^T}_{\tau i}(\boldsymbol{F}_\tau\boldsymbol{g}_i)^T\left\{(\boldsymbol{D}_p)^T\left[\widetilde{\boldsymbol{C}}^k_{pn}\boldsymbol{D}_{nz}(\boldsymbol{F}_s\boldsymbol{g}_j)\right]\right\}\boldsymbol{U}^k_{sj}d\Omega^k dz \\
&-\int_{\Omega^k}\int_{A^k}\delta\boldsymbol{U}^{k^T}_{\tau i}(\boldsymbol{F}_\tau\boldsymbol{g}_i)^T\left\{(\boldsymbol{D}_{np})^T\left[\widetilde{\boldsymbol{C}}^k_{np}\boldsymbol{D}_p(\boldsymbol{F}_s\boldsymbol{g}_j)\right]\right\}\boldsymbol{U}^k_{sj}d\Omega^k dz \\
&-\int_{\Omega^k}\int_{A^k}\delta\boldsymbol{U}^{k^T}_{\tau i}(\boldsymbol{F}_\tau\boldsymbol{g}_i)^T\left\{(\boldsymbol{D}_{np})^T\left[\widetilde{\boldsymbol{C}}^k_{nn}\boldsymbol{D}_{np}(\boldsymbol{F}_s\boldsymbol{g}_j)\right]\right\}\boldsymbol{U}^k_{sj}d\Omega^k dz \\
&-\int_{\Omega^k}\int_{A^k}\delta\boldsymbol{U}^{k^T}_{\tau i}(\boldsymbol{F}_\tau\boldsymbol{g}_i)^T\left\{(\boldsymbol{D}_{np})^T\left[\widetilde{\boldsymbol{C}}^k_{nn}\boldsymbol{D}_{nz}(\boldsymbol{F}_s\boldsymbol{g}_j)\right]\right\}\boldsymbol{U}^k_{sj}d\Omega^k dz \\
&-\int_{\Omega^k}\int_{A^k}\delta\boldsymbol{U}^{k^T}_{\tau i}(\boldsymbol{F}_\tau\boldsymbol{g}_i)^T\left\{(\boldsymbol{D}_{nz})^T\left[\widetilde{\boldsymbol{C}}^k_{np}\boldsymbol{D}_p(\boldsymbol{F}_s\boldsymbol{g}_j)\right]\right\}\boldsymbol{U}^k_{sj}d\Omega^k dz \\
&-\int_{\Omega^k}\int_{A^k}\delta\boldsymbol{U}^{k^T}_{\tau i}(\boldsymbol{F}_\tau\boldsymbol{g}_i)^T\left\{(\boldsymbol{D}_{nz})^T\left[\widetilde{\boldsymbol{C}}^k_{nn}\boldsymbol{D}_{np}(\boldsymbol{F}_s\boldsymbol{g}_j)\right]\right\}\boldsymbol{U}^k_{sj}d\Omega^k dz \\
&-\int_{\Omega^k}\int_{A^k}\delta\boldsymbol{U}^{k^T}_{\tau i}(\boldsymbol{F}_\tau\boldsymbol{g}_i)^T\left\{(\boldsymbol{D}_{nz})^T\left[\widetilde{\boldsymbol{C}}^k_{nn}\boldsymbol{D}_{nz}(\boldsymbol{F}_s\boldsymbol{g}_j)\right]\right\}\boldsymbol{U}^k_{sj}d\Omega^k dz \\
&+\int_{\Gamma^k}\int_{A^k}\delta\boldsymbol{U}^{k^T}_{\tau i}(\boldsymbol{F}_\tau\boldsymbol{g}_i)^T\left\{(\boldsymbol{I}_p)^T\left[\widetilde{\boldsymbol{C}}^k_{pp}\boldsymbol{D}_p(\boldsymbol{F}_s\boldsymbol{g}_j)\right]\right\}\boldsymbol{U}^k_{sj}d\Gamma^k dz \\
&+\int_{\Gamma^k}\int_{A^k}\delta\boldsymbol{U}^{k^T}_{\tau i}(\boldsymbol{F}_\tau\boldsymbol{g}_i)^T\left\{(\boldsymbol{I}_p)^T\left[\widetilde{\boldsymbol{C}}^k_{pn}\boldsymbol{D}_{np}(\boldsymbol{F}_s\boldsymbol{g}_j)\right]\right\}\boldsymbol{U}^k_{sj}d\Gamma^k dz \\
&+\int_{\Gamma^k}\int_{A^k}\delta\boldsymbol{U}^{k^T}_{\tau i}(\boldsymbol{F}_\tau\boldsymbol{g}_i)^T\left\{(\boldsymbol{I}_p)^T\left[\widetilde{\boldsymbol{C}}^k_{pn}\boldsymbol{D}_{nz}(\boldsymbol{F}_s\boldsymbol{g}_j)\right]\right\}\boldsymbol{U}^k_{sj}d\Gamma^k dz
\end{aligned}$$

$$
\begin{aligned}
&+\int_{\Gamma^k}\int_{A^k}\delta\boldsymbol{U}_{\tau i}^{k^T}(\boldsymbol{F}_\tau\mathbf{g}_i)^T\Big\{(\boldsymbol{I}_{np})^T\Big[\widetilde{\boldsymbol{C}}_{np}^k\boldsymbol{D}_p(\boldsymbol{F}_s\mathbf{g}_j)\Big]\Big\}\boldsymbol{U}_{sj}^k d\Gamma^k\,dz\\
&+\int_{\Gamma^k}\int_{A^k}\delta\boldsymbol{U}_{\tau i}^{k^T}(\boldsymbol{F}_\tau\mathbf{g}_i)^T\Big\{(\boldsymbol{I}_{np})^T\Big[\widetilde{\boldsymbol{C}}_{nn}^k\boldsymbol{D}_{np}(\boldsymbol{F}_s\mathbf{g}_j)\Big]\Big\}\boldsymbol{U}_{sj}^k d\Gamma^k\,dz\\
&+\int_{\Gamma^k}\int_{A^k}\delta\boldsymbol{U}_{\tau i}^{k^T}(\boldsymbol{F}_\tau\mathbf{g}_i)^T\Big\{(\boldsymbol{I}_{np})^T\Big[\widetilde{\boldsymbol{C}}_{nn}^k\boldsymbol{D}_{nz}(\boldsymbol{F}_s\mathbf{g}_j)\Big]\Big\}\boldsymbol{U}_{sj}^k d\Gamma^k\,dz
\end{aligned}
\tag{59}
$$

where

$$
\boldsymbol{I}_p=\begin{bmatrix}1&0&0\\0&1&0\\1&1&0\end{bmatrix};\quad \boldsymbol{I}_{np}=\begin{bmatrix}0&0&1\\0&0&1\\0&0&0\end{bmatrix};
\tag{60}
$$

By considering the functional in Eq. (59) the *stiffness and boundary nuclei* can be obtained. If only the stiffness nucleus is taken into account then *classical Galerkin method* is performed, if also the boundary nucleus is introduced in the analysis then *Generalized Galerkin method* is carried out. It should be noted that if the functional in Eq. (59) is used, then an higher differentiability grade, for the basis functions $\mathbf{g}_i$, is required. This is the main and substantial difference between Ritz and Galerkin methods. When for particular boundary conditions or lamination angles the boundary terms are not zero then Generalized Galerkin method becomes extremely useful. The functional in Eq. (59) should be used both to obtain the Galerkin stiffness nucleus, with related boundary nucleus, and to obtain the differential governing equations with variationally consistent boundary conditions. The Galerkin stiffness and boundary nuclei assume the following form:

$$
\begin{aligned}
\boldsymbol{K}^{k\tau sij}=&\int_{\Omega^k}\int_{A^k}\Big(-(\boldsymbol{F}_\tau\mathbf{g}_i)^T\Big\{(\boldsymbol{D}_p)^T\Big[\widetilde{\boldsymbol{C}}_{pp}^k\boldsymbol{D}_p(\boldsymbol{F}_s\mathbf{g}_j)\\
&+\widetilde{\boldsymbol{C}}_{pn}^k\boldsymbol{D}_{np}(\boldsymbol{F}_s\mathbf{g}_j)+\widetilde{\boldsymbol{C}}_{pn}^k\boldsymbol{D}_{nz}(\boldsymbol{F}_s\mathbf{g}_j)\Big]\Big\}\\
&-(\boldsymbol{F}_\tau\mathbf{g}_i)^T\Big\{(\boldsymbol{D}_{np})^T\Big[\widetilde{\boldsymbol{C}}_{np}^k\boldsymbol{D}_p(\boldsymbol{F}_s\mathbf{g}_j)\\
&+\widetilde{\boldsymbol{C}}_{nn}^k\boldsymbol{D}_{np}(\boldsymbol{F}_s\mathbf{g}_j)\\
&+\widetilde{\boldsymbol{C}}_{nn}^k\boldsymbol{D}_{nz}(\boldsymbol{F}_s\mathbf{g}_j)\Big]\Big\}\\
&+(\boldsymbol{F}_\tau\mathbf{g}_i)^T\Big\{(\boldsymbol{D}_{nz})^T\Big[\widetilde{\boldsymbol{C}}_{np}^k\boldsymbol{D}_p(\boldsymbol{F}_s\mathbf{g}_j)\\
&+\widetilde{\boldsymbol{C}}_{nn}^k\boldsymbol{D}_{np}(\boldsymbol{F}_s\mathbf{g}_j)+\widetilde{\boldsymbol{C}}_{nn}^k\boldsymbol{D}_{nz}(\boldsymbol{F}_s\mathbf{g}_j)\Big]\Big\}\Big)d\Omega^k\,dz\\
\boldsymbol{\Pi}^{k\tau sij}=&\int_{\Gamma^k}\int_{A^k}\Big((\boldsymbol{F}_\tau\mathbf{g}_i)^T\Big\{(\boldsymbol{I}_p)^T\Big[\widetilde{\boldsymbol{C}}_{pp}^k\boldsymbol{D}_p(\boldsymbol{F}_s\mathbf{g}_j)\\
&+\widetilde{\boldsymbol{C}}_{pn}^k\boldsymbol{D}_{np}(\boldsymbol{F}_\tau\mathbf{g}_j)+\widetilde{\boldsymbol{C}}_{pn}^k\boldsymbol{D}_{nz}(\boldsymbol{F}_\tau\mathbf{g}_j)\Big]\Big\}\\
&+(\boldsymbol{F}_\tau\mathbf{g}_i)^T\Big\{(\boldsymbol{I}_{np})^T\Big[\widetilde{\boldsymbol{C}}_{np}^k\boldsymbol{D}_p(\boldsymbol{F}_s\mathbf{g}_j)\\
&+\widetilde{\boldsymbol{C}}_{nn}^k\boldsymbol{D}_{np}(\boldsymbol{F}_s\mathbf{g}_j)\\
&+\widetilde{\boldsymbol{C}}_{nn}^k\boldsymbol{D}_{nz}(\boldsymbol{F}_s\mathbf{g}_j)\Big]\Big\}\Big)d\Gamma^k\,dz
\end{aligned}
\tag{61}
$$

performing the matrix calculus in Eq. (61), the 9 stiffness secondary nuclei become:

$$
\begin{aligned}
K_{u_xu_x}^{\tau_{u_x}s_{u_x}}=&\widetilde{\boldsymbol{C}}_{11}^k\Big[\int_{A^k}(F_{\tau_{u_x}}F_{s_{u_x}})dz\Big]\Big[\int_{\Omega^k}(\psi_{x_i}\psi_{x_j,xx})d\Omega^k\Big]\\
&+\widetilde{\boldsymbol{C}}_{16}^k\Big[\int_{A^k}(F_{\tau_{u_x}}F_{s_{u_x}})dz\Big]\Big[\int_{\Omega^k}(\psi_{x_i}\psi_{x_j,xy})d\Omega^k\Big]\\
&+\widetilde{\boldsymbol{C}}_{16}^k\Big[\int_{A^k}(F_{\tau_{u_x}}F_{s_{u_x}})dz\Big]\Big[\int_{\Omega^k}(\psi_{x_i}\psi_{x_j,yx})d\Omega^k\Big]\\
&+\widetilde{\boldsymbol{C}}_{66}^k\Big[\int_{A^k}(F_{\tau_{u_x}}F_{s_{u_x}})dz\Big]\Big[\int_{\Omega^k}(\psi_{x_i}\psi_{x_j,yy})d\Omega^k\Big]\\
&+\widetilde{\boldsymbol{C}}_{55}^k\Big[\int_{A^k}(F_{\tau_{u_x,z}}F_{s_{u_x,z}})dz\Big]\Big[\int_{\Omega^k}(\psi_{x_i}\psi_{x_j})d\Omega^k\Big]
\end{aligned}
$$

$$
\begin{aligned}
K_{u_xu_y}^{\tau_{u_x}s_{u_y}}=&\widetilde{\boldsymbol{C}}_{16}^k\Big[\int_{A^k}(F_{\tau_{u_x}}F_{s_{u_y}})dz\Big]\Big[\int_{\Omega^k}(\psi_{x_i}\psi_{y_j,xx})d\Omega^k\Big]\\
&+\widetilde{\boldsymbol{C}}_{12}^k\Big[\int_{A^k}(F_{\tau_{u_x}}F_{s_{u_y}})dz\Big]\Big[\int_{\Omega^k}(\psi_{x_i}\psi_{y_j,xy})d\Omega^k\Big]\\
&+\widetilde{\boldsymbol{C}}_{66}^k\Big[\int_{A^k}(F_{\tau_{u_x}}F_{s_{u_y}})dz\Big]\Big[\int_{\Omega^k}(\psi_{x_i}\psi_{y_j,yx})d\Omega^k\Big]\\
&+\widetilde{\boldsymbol{C}}_{26}^k\Big[\int_{A^k}(F_{\tau_{u_x}}F_{s_{u_y}})dz\Big]\Big[\int_{\Omega^k}(\psi_{x_i}\psi_{y_j,yy})d\Omega^k\Big]\\
&+\widetilde{\boldsymbol{C}}_{45}^k\Big[\int_{A^k}(F_{\tau_{u_x,z}}F_{s_{u_y,z}})dz\Big]\Big[\int_{\Omega^k}(\psi_{x_i}\psi_{y_j})d\Omega^k\Big]\\
K_{u_xu_z}^{\tau_{u_x}s_{u_z}}=&\widetilde{\boldsymbol{C}}_{55}^k\Big[\int_{A^k}(F_{\tau_{u_x,z}}F_{s_{u_z}})dz\Big]\Big[\int_{\Omega^k}(\psi_{x_i}\psi_{z_j,x})d\Omega^k\Big]\\
&+\widetilde{\boldsymbol{C}}_{45}^k\Big[\int_{A^k}(F_{\tau_{u_x,z}}F_{s_{u_z}})dz\Big]\Big[\int_{\Omega^k}(\psi_{x_i}\psi_{z_j,y})d\Omega^k\Big]\\
&+\widetilde{\boldsymbol{C}}_{13}^k\Big[\int_{A^k}(F_{\tau_{u_x}}F_{s_{u_z,z}})dz\Big]\Big[\int_{\Omega^k}(\psi_{x_i,x}\psi_{z_j})d\Omega^k\Big]\\
&+\widetilde{\boldsymbol{C}}_{36}^k\Big[\int_{A^k}(F_{\tau_{u_x}}F_{s_{u_z,z}})dz\Big]\Big[\int_{\Omega^k}(\psi_{x_i,y}\psi_{z_j})d\Omega^k\Big]\\
K_{u_yu_x}^{\tau_{u_y}s_{u_x}}=&\widetilde{\boldsymbol{C}}_{16}^k\Big[\int_{A^k}(F_{\tau_{u_y}}F_{s_{u_x}})dz\Big]\Big[\int_{\Omega^k}(\psi_{x_i}\psi_{y_j,xx})d\Omega^k\Big]\\
&+\widetilde{\boldsymbol{C}}_{12}^k\Big[\int_{A^k}(F_{\tau_{u_y}}F_{s_{u_x}})dz\Big]\Big[\int_{\Omega^k}(\psi_{x_i}\psi_{y_j,xy})d\Omega^k\Big]\\
&+\widetilde{\boldsymbol{C}}_{66}^k\Big[\int_{A^k}(F_{\tau_{u_y}}F_{s_{u_x}})dz\Big]\Big[\int_{\Omega^k}(\psi_{x_i}\psi_{y_j,yx})d\Omega^k\Big]\\
&+\widetilde{\boldsymbol{C}}_{26}^k\Big[\int_{A^k}(F_{\tau_{u_y}}F_{s_{u_x}})dz\Big]\Big[\int_{\Omega^k}(\psi_{x_i}\psi_{y_j,yy})d\Omega^k\Big]\\
&+\widetilde{\boldsymbol{C}}_{45}^k\Big[\int_{A^k}(F_{\tau_{u_y,z}}F_{s_{u_x,z}})dz\Big]\Big[\int_{\Omega^k}(\psi_{x_i}\psi_{y_j})d\Omega^k\Big]\\
K_{u_yu_y}^{\tau_{u_y}s_{u_y}}=&\widetilde{\boldsymbol{C}}_{26}^k\Big[\int_{A^k}(F_{\tau_{u_y}}F_{s_{u_y}})dz\Big]\Big[\int_{\Omega^k}(\psi_{y_i,y}\psi_{y_j,x})d\Omega^k\Big]\\
&+\widetilde{\boldsymbol{C}}_{22}^k\Big[\int_{A^k}(F_{\tau_{u_y}}F_{s_{u_y}})dz\Big]\Big[\int_{\Omega^k}(\psi_{y_i}\psi_{y_j,yy})d\Omega^k\Big]\\
&+\widetilde{\boldsymbol{C}}_{66}^k\Big[\int_{A^k}(F_{\tau_{u_y}}F_{s_{u_y}})dz\Big]\Big[\int_{\Omega^k}(\psi_{y_i},\psi_{y_j,xy})d\Omega^k\Big]\\
&+\widetilde{\boldsymbol{C}}_{26}^k\Big[\int_{A^k}(F_{\tau_{u_y}}F_{s_{u_y}})dz\Big]\Big[\int_{\Omega^k}(\psi_{y_i}\psi_{y_j,yy})d\Omega^k\Big]\\
&+\widetilde{\boldsymbol{C}}_{44}^k\Big[\int_{A^k}(F_{\tau_{u_y,z}}F_{s_{u_y,z}})dz\Big]\Big[\int_{\Omega^k}(\psi_{y_i}\psi_{y_j})d\Omega^k\Big]\\
K_{u_yu_z}^{\tau_{u_y}s_{u_z}}=&\widetilde{\boldsymbol{C}}_{45}^k\Big[\int_{A^k}(F_{\tau_{u_y,z}}F_{s_{u_z}})dz\Big]\Big[\int_{\Omega^k}(\psi_{y_i}\psi_{z_j,x})d\Omega^k\Big]\\
&+\widetilde{\boldsymbol{C}}_{44}^k\Big[\int_{A^k}(F_{\tau_{u_y,z}}F_{s_{u_z}})dz\Big]\Big[\int_{\Omega^k}(\psi_{y_i}\psi_{z_j,y})d\Omega^k\Big]\\
&+\widetilde{\boldsymbol{C}}_{36}^k\Big[\int_{A^k}(F_{\tau_{u_y}}F_{s_{u_z,z}})dz\Big]\Big[\int_{\Omega^k}(\psi_{y_i,x}\psi_{z_j})d\Omega^k\Big]\\
&+\widetilde{\boldsymbol{C}}_{23}^k\Big[\int_{A^k}(F_{\tau_{u_y}}F_{s_{u_z,z}})dz\Big]\Big[\int_{\Omega^k}(\psi_{y_i,y}\psi_{z_j})d\Omega^k\Big]\\
K_{u_zu_x}^{\tau_{u_z}s_{u_x}}=&\widetilde{\boldsymbol{C}}_{55}^k\Big[\int_{A^k}(F_{\tau_{u_z}}F_{s_{u_x,z}})dz\Big]\Big[\int_{\Omega^k}(\psi_{x_i}\psi_{z_j,x})d\Omega^k\Big]\\
&+\widetilde{\boldsymbol{C}}_{45}^k\Big[\int_{A^k}(F_{\tau_{u_z}}F_{s_{u_x,z}})dz\Big]\Big[\int_{\Omega^k}(\psi_{x_i}\psi_{z_j,y})d\Omega^k\Big]\\
&+\widetilde{\boldsymbol{C}}_{13}^k\Big[\int_{A^k}(F_{\tau_{u_z,z}}F_{s_{u_x}})dz\Big]\Big[\int_{\Omega^k}(\psi_{x_i,x}\psi_{z_j})d\Omega^k\Big]\\
&+\widetilde{\boldsymbol{C}}_{36}^k\Big[\int_{A^k}(F_{\tau_{u_z,z}}F_{s_{u_x}})dz\Big]\Big[\int_{\Omega^k}(\psi_{x_i,y}\psi_{z_j})d\Omega^k\Big]
\end{aligned}
$$

$$
\begin{aligned}
K_{u_z u_y}^{\tau_{u_z} s_{u_y}} &= \widetilde{\boldsymbol{C}}_{45}^k \left[\int_{A^k} (F_{\tau_{u_z}} F_{s_{u_y,z}}) dz\right] \left[\int_{\Omega^k} (\psi_{y_i} \psi_{z_j,x}) d\Omega^k\right] \\
&\quad + \widetilde{\boldsymbol{C}}_{44}^k \left[\int_{A^k} (F_{\tau_{u_z}} F_{s_{u_y,z}}) dz\right] \left[\int_{\Omega^k} (\psi_{y_i} \psi_{z_j,y}) d\Omega^k\right] \\
&\quad + \widetilde{\boldsymbol{C}}_{36}^k \left[\int_{A^k} (F_{\tau_{u_z,z}} F_{s_{u_y}}) dz\right] \left[\int_{\Omega^k} (\psi_{y_i,x} \psi_{z_j}) d\Omega^k\right] \\
&\quad + \widetilde{\boldsymbol{C}}_{23}^k \left[\int_{A^k} (F_{\tau_{u_z,z}} F_{s_{u_y}}) dz\right] \left[\int_{\Omega^k} (\psi_{y_i,y} \psi_{z_j}) d\Omega^k\right] \\
K_{u_z u_z}^{\tau_{u_z} s_{u_z}} &= \widetilde{\boldsymbol{C}}_{45}^k \left[\int_{A^k} (F_{\tau_{u_z}} F_{s_{u_z}}) dz\right] \left[\int_{\Omega^k} (\psi_{z_i,y} \psi_{z_j,x}) d\Omega^k\right] \\
&\quad + \widetilde{\boldsymbol{C}}_{44}^k \left[\int_{A^k} (F_{\tau_{u_z}} F_{s_{u_z}}) dz\right] \left[\int_{\Omega^k} (\psi_{z_i} \psi_{z_j,yy}) d\Omega^k\right] \\
&\quad + \widetilde{\boldsymbol{C}}_{55}^k \left[\int_{A^k} (F_{\tau_{u_z}} F_{s_{u_z}}) dz\right] \left[\int_{\Omega^k} (\psi_{z_i} \psi_{z_j,xx}) d\Omega^k\right] \\
&\quad + \widetilde{\boldsymbol{C}}_{45}^k \left[\int_{A^k} (F_{\tau_{u_z}} F_{s_{u_z}}) dz\right] \left[\int_{\Omega^k} (\psi_{z_i} \psi_{z_j,yx}) d\Omega^k\right] \\
&\quad + \widetilde{\boldsymbol{C}}_{33}^k \left[\int_{A^k} (F_{\tau_{u_z,z}} F_{s_{u_z,z}}) dz\right] \left[\int_{\Omega^k} (\psi_{z_i} \psi_{z_j}) d\Omega^k\right]
\end{aligned} \tag{62}
$$

and the 9 boundary secondary nuclei are:

$$
\begin{aligned}
\Pi_{u_x u_x}^{\tau_{u_x} s_{u_x}} &= \widetilde{\boldsymbol{C}}_{11}^k \left[\int_{A^k} (F_{\tau_{u_x}} F_{s_{u_x}}) dz\right] \left[\int_{\Gamma^k} (\psi_{x_i,x} \psi_{x_j}) d\Gamma^k\right] \\
&\quad + \widetilde{\boldsymbol{C}}_{16}^k \left[\int_{A^k} (F_{\tau_{u_x}} F_{s_{u_x}}) dz\right] \left[\int_{\Gamma^k} (\psi_{x_i,x} \psi_{x_j}) d\Gamma^k\right] \\
&\quad + \widetilde{\boldsymbol{C}}_{16}^k \left[\int_{A^k} (F_{\tau_{u_x}} F_{s_{u_x}}) dz\right] \left[\int_{\Gamma^k} (\psi_{x_i,y} \psi_{x_j}) d\Gamma^k\right] \\
&\quad + \widetilde{\boldsymbol{C}}_{66}^k \left[\int_{A^k} (F_{\tau_{u_x}} F_{s_{u_x}}) dz\right] \left[\int_{\Gamma^k} (\psi_{x_i,y} \psi_{x_j}) d\Gamma^k\right] \\
\Pi_{u_x u_y}^{\tau_{u_x} s_{u_y}} &= \widetilde{\boldsymbol{C}}_{12}^k \left[\int_{A^k} (F_{\tau_{u_x}} F_{s_{u_y}}) dz\right] \left[\int_{\Gamma^k} (\psi_{x_i,y} \psi_{y_j}) d\Gamma^k\right] \\
&\quad + \widetilde{\boldsymbol{C}}_{16}^k \left[\int_{A^k} (F_{\tau_{u_x}} F_{s_{u_y}}) dz\right] \left[\int_{\Gamma^k} (\psi_{x_i,x} \psi_{y_j}) d\Gamma^k\right] \\
&\quad + \widetilde{\boldsymbol{C}}_{26}^k \left[\int_{A^k} (F_{\tau_{u_x}} F_{s_{u_y}}) dz\right] \left[\int_{\Gamma^k} (\psi_{x_i,y} \psi_{y_j}) d\Gamma^k\right] \\
&\quad + \widetilde{\boldsymbol{C}}_{66}^k \left[\int_{A^k} (F_{\tau_{u_x}} F_{s_{u_y}}) dz\right] \left[\int_{\Gamma^k} (\psi_{x_i,x} \psi_{y_j}) d\Gamma^k\right] \\
\Pi_{u_x u_z}^{\tau_{u_x} s_{u_z}} &= \widetilde{\boldsymbol{C}}_{13}^k \left[\int_{A^k} (F_{\tau_{u_x}} F_{s_{u_z,z}}) dz\right] \left[\int_{\Gamma^k} (\psi_{x_i,x} \psi_{z_j}) d\Gamma^k\right] \\
&\quad + \widetilde{\boldsymbol{C}}_{36}^k \left[\int_{A^k} (F_{\tau_{u_x}} F_{s_{u_z,z}}) dz\right] \left[\int_{\Gamma^k} (\psi_{x_i,y} \psi_{z_j}) d\Gamma^k\right] \\
\Pi_{u_y u_x}^{\tau_{u_y} s_{u_x}} &= \widetilde{\boldsymbol{C}}_{12}^k \left[\int_{A^k} (F_{\tau_{u_y}} F_{s_{u_x}}) dz\right] \left[\int_{\Gamma^k} (\psi_{x_i,x} \psi_{y_j}) d\Gamma^k\right] \\
&\quad + \widetilde{\boldsymbol{C}}_{16}^k \left[\int_{A^k} (F_{\tau_{u_y}} F_{s_{u_x}}) dz\right] \left[\int_{\Gamma^k} (\psi_{x_i,x} \psi_{y_j}) d\Gamma^k\right] \\
&\quad + \widetilde{\boldsymbol{C}}_{26}^k \left[\int_{A^k} (F_{\tau_{u_y}} F_{s_{u_x}}) dz\right] \left[\int_{\Gamma^k} (\psi_{x_i,y} \psi_{y_j}) d\Gamma^k\right] \\
&\quad + \widetilde{\boldsymbol{C}}_{66}^k \left[\int_{A^k} (F_{\tau_{u_y}} F_{s_{u_x}}) dz\right] \left[\int_{\Gamma^k} (\psi_{x_i,y} \psi_{y_j}) d\Gamma^k\right] \\
\Pi_{u_y u_y}^{\tau_{u_y} s_{u_y}} &= \widetilde{\boldsymbol{C}}_{22}^k \left[\int_{A^k} (F_{\tau_{u_y}} F_{s_{u_y}}) dz\right] \left[\int_{\Gamma^k} (\psi_{y_i,y} \psi_{y_j}) d\Gamma^k\right] \\
&\quad + \widetilde{\boldsymbol{C}}_{26}^k \left[\int_{A^k} (F_{\tau_{u_y}} F_{s_{u_y}}) dz\right] \left[\int_{\Gamma^k} (\psi_{y_i,x} \psi_{y_j}) d\Gamma^k\right] \\
&\quad + \widetilde{\boldsymbol{C}}_{26}^k \left[\int_{A^k} (F_{\tau_{u_y}} F_{s_{u_y}}) dz\right] \left[\int_{\Gamma^k} (\psi_{y_i,y} \psi_{y_j}) d\Gamma^k\right] \\
&\quad + \widetilde{\boldsymbol{C}}_{66}^k \left[\int_{A^k} (F_{\tau_{u_y}} F_{s_{u_y}}) dz\right] \left[\int_{\Gamma^k} (\psi_{y_i,x} \psi_{y_j}) d\Gamma^k\right] \\
\Pi_{u_y u_z}^{\tau_{u_y} s_{u_z}} &= \widetilde{\boldsymbol{C}}_{23}^k \left[\int_{A^k} (F_{\tau_{u_y}} F_{s_{u_z,z}}) dz\right] \left[\int_{\Gamma^k} (\psi_{z_i} \psi_{y_j}) d\Gamma^k\right] \\
&\quad + \widetilde{\boldsymbol{C}}_{36}^k \left[\int_{A^k} (F_{\tau_{u_y}} F_{s_{u_z,z}}) dz\right] \left[\int_{\Gamma^k} (\psi_{z_i} \psi_{y_j}) d\Gamma^k\right] \\
\Pi_{u_z u_x}^{\tau_{u_z} s_{u_x}} &= \widetilde{\boldsymbol{C}}_{45}^k \left[\int_{A^k} (F_{\tau_{u_z}} F_{s_{u_x,z}}) dz\right] \left[\int_{\Gamma^k} (\psi_{x_i} \psi_{z_j}) d\Gamma^k\right] \\
&\quad + \widetilde{\boldsymbol{C}}_{55}^k \left[\int_{A^k} (F_{\tau_{u_z}} F_{s_{u_x,z}}) dz\right] \left[\int_{\Gamma^k} (\psi_{x_i} \psi_{z_j}) d\Gamma^k\right] \\
\Pi_{u_z u_y}^{\tau_{u_z} s_{u_y}} &= \widetilde{\boldsymbol{C}}_{44}^k \left[\int_{A^k} (F_{\tau_{u_z}} F_{s_{u_y,z}}) dz\right] \left[\int_{\Gamma^k} (\psi_{y_i} \psi_{z_j}) d\Gamma^k\right] \\
&\quad + \widetilde{\boldsymbol{C}}_{45}^k \left[\int_{A^k} (F_{\tau_{u_z}} F_{s_{u_y,z}}) dz\right] \left[\int_{\Gamma^k} (\psi_{y_i} \psi_{z_j}) d\Gamma^k\right] \\
\Pi_{u_z u_z}^{\tau_{u_z} s_{u_z}} &= \widetilde{\boldsymbol{C}}_{44}^k \left[\int_{A^k} (F_{\tau_{u_z}} F_{s_{u_z}}) dz\right] \left[\int_{\Gamma^k} (\psi_{z_i,y} \psi_{z_j}) d\Gamma^k\right] \\
&\quad + \widetilde{\boldsymbol{C}}_{45}^k \left[\int_{A^k} (F_{\tau_{u_z}} F_{s_{u_z}}) dz\right] \left[\int_{\Gamma^k} (\psi_{z_i,x} \psi_{z_j}) d\Gamma^k\right] \\
&\quad + \widetilde{\boldsymbol{C}}_{45}^k \left[\int_{A^k} (F_{\tau_{u_z}} F_{s_{u_z}}) dz\right] \left[\int_{\Gamma^k} (\psi_{z_i,y} \psi_{z_j}) d\Gamma^k\right] \\
&\quad + \widetilde{\boldsymbol{C}}_{55}^k \left[\int_{A^k} (F_{\tau_{u_z}} F_{s_{u_z}}) dz\right] \left[\int_{\Gamma^k} (\psi_{z_i,x} \psi_{z_j}) d\Gamma^k\right]
\end{aligned} \tag{63}
$$

both stiffness and boundary main nuclei are composed of 9 invariant secondary nuclei, which after the expansion according to the used theory assume the following form:

$$
\boldsymbol{K}^{k\tau sij} = \begin{bmatrix} \boldsymbol{K}_{u_x u_x} & \boldsymbol{K}_{u_x u_y} & \boldsymbol{K}_{u_x u_z} \\ \boldsymbol{K}_{u_y u_x} & \boldsymbol{K}_{u_y u_y} & \boldsymbol{K}_{u_y u_z} \\ \boldsymbol{K}_{u_z u_x} & \boldsymbol{K}_{u_z u_y} & \boldsymbol{K}_{u_z u_z} \end{bmatrix}, \quad \boldsymbol{\Pi}^{k\tau sij} = \begin{bmatrix} \boldsymbol{\Pi}_{u_x u_x} & \boldsymbol{\Pi}_{u_x u_y} & \boldsymbol{\Pi}_{u_x u_z} \\ \boldsymbol{\Pi}_{u_y u_x} & \boldsymbol{\Pi}_{u_y u_y} & \boldsymbol{\Pi}_{u_y u_z} \\ \boldsymbol{\Pi}_{u_z u_x} & \boldsymbol{\Pi}_{u_z u_y} & \boldsymbol{\Pi}_{u_z u_z} \end{bmatrix} \tag{64}
$$

If the Galerkin method is applied to the total potential energy functional in Eq. (33) then the results are perfectly coincident with Ritz method. It should be observed that if the boundary terms are zero the three different methodologies lead to the same results, this is true, for isotropic and cross-ply laminates with simply supported boundary condition. On the contrary if the lamination schemes are angle-ply or the boundary conditions are not simply supported, then the boundary terms give a contribution that has to be taken into consideration by using Generalized Galerkin method. The advantage to use Galerkin method is that only the governing differential equations are required and the boundary condition are negligible. Nevertheless, when the boundary terms are not zero, the stiffness matrix can lose some important proprieties like symmetry and positivity-definite. This is extremely important from a computation point of view, above all increasing the value of the half-waves m, n. Indeed in these cases some algorithms for the calculation of the eigenvalues which are computationally more expensive have to be used.

5. Governing equations

By imposing the condition in Eq. (59) at the functional in Eq. (34), then the differential governing equations with variationally consistent boundary conditions are obtained:

$$
\begin{aligned}
&\delta \boldsymbol{u}_\tau^k : \boldsymbol{K}_d^{k\tau s} \boldsymbol{u}_s^k = \boldsymbol{M}^{k\tau s} \ddot{\boldsymbol{u}}_s^k + \boldsymbol{K}_\sigma^{k\tau s} \boldsymbol{u}_s^k \\
&\text{geometrical on } \Gamma_g^k \quad \text{mechanical on } \Gamma_m^k \\
&\boldsymbol{u}_\tau^k = \bar{\boldsymbol{u}}_\tau^k \quad \boldsymbol{\Pi}_d^{k\tau s} \boldsymbol{u}_s^k = \boldsymbol{\Pi}_d^{k\tau s} \bar{\boldsymbol{u}}_s^k
\end{aligned} \tag{65}
$$

where

$$
\begin{aligned}
\boldsymbol{K}_d^{k\tau s} = & \int_{A^k}\Big(-(\boldsymbol{F}_\tau)^T\Big\{(\boldsymbol{D}_p)^T\Big[\widetilde{\boldsymbol{C}}_{pp}^k\boldsymbol{D}_p(\boldsymbol{F}_\tau)+\widetilde{\boldsymbol{C}}_{pn}^k\boldsymbol{D}_{np}(\boldsymbol{F}_\tau)+\widetilde{\boldsymbol{C}}_{pn}^k\boldsymbol{D}_{nz}(\boldsymbol{F}_\tau)\Big]\Big\}\\
& -(\boldsymbol{F}_\tau)^T\Big\{(\boldsymbol{D}_{np})^T\Big[\widetilde{\boldsymbol{C}}_{np}^k\boldsymbol{D}_p(\boldsymbol{F}_\tau)+\widetilde{\boldsymbol{C}}_{nn}^k\boldsymbol{D}_{np}(\boldsymbol{F}_\tau)+\widetilde{\boldsymbol{C}}_{nn}^k\boldsymbol{D}_{nz}(\boldsymbol{F}_\tau)\Big]\Big\}\\
& +(\boldsymbol{F}_\tau)^T\Big\{(\boldsymbol{D}_{nz})^T\Big[\widetilde{\boldsymbol{C}}_{np}^k\boldsymbol{D}_p(\boldsymbol{F}_\tau)+\widetilde{\boldsymbol{C}}_{nn}^k\boldsymbol{D}_{np}(\boldsymbol{F}_\tau)+\widetilde{\boldsymbol{C}}_{nn}^k\boldsymbol{D}_{nz}(\boldsymbol{F}_\tau)\Big]\Big\}\Big)dz\\
\boldsymbol{\Pi}_d^{k\tau s} = & \int_{A^k}((\boldsymbol{F}_\tau)^T\Big\{(\boldsymbol{I}_p)^T\Big[\widetilde{\boldsymbol{C}}_{pp}^k\boldsymbol{D}_p(\boldsymbol{F}_\tau)+\widetilde{\boldsymbol{C}}_{pn}^k\boldsymbol{D}_{np}(\boldsymbol{F}_\tau)+\widetilde{\boldsymbol{C}}_{pn}^k\boldsymbol{D}_{nz}(\boldsymbol{F}_\tau)\Big]\Big\}\\
& +(\boldsymbol{F}_\tau)^T\Big\{(\boldsymbol{I}_{np})^T\Big[\widetilde{\boldsymbol{C}}_{np}^k\boldsymbol{D}_p(\boldsymbol{F}_\tau)+\widetilde{\boldsymbol{C}}_{nn}^k\boldsymbol{D}_{np}(\boldsymbol{F}_\tau)+\widetilde{\boldsymbol{C}}_{nn}^k\boldsymbol{D}_{nz}(\boldsymbol{F}_\tau)\Big]\Big\})dz\\
\boldsymbol{M}^{k\tau s} = & \int_{A^k}\rho^k(\boldsymbol{F}_\tau)^T(\boldsymbol{F}_s)dz\\
\boldsymbol{K}_\sigma^{k\tau s}(1,1) = & \,\delta_v\Big(\sigma_{xx_0}^k\Big[\int_{A^k}F_{\tau_{u_x}}F_{s_{u_x}}\,dz\Big]\partial_x^2 + \sigma_{yy_0}^k\Big[\int_{A^k}F_{\tau_{u_x}}F_{s_{u_x}}\,dz\Big]\partial_y^2 + 2\sigma_{xy_0}^k\Big[\int_{A^k}F_{\tau_{u_x}}F_{s_{u_x}}\,dz\Big]\partial_{xy}^2\Big)\\
\boldsymbol{K}_\sigma^{k\tau s}(2,2) = & \,\delta_v\Big(\sigma_{xx_0}^k\Big[\int_{A^k}F_{\tau_{u_y}}F_{s_{u_y}}\,dz\Big]\partial_x^2 + \sigma_{yy_0}^k\Big[\int_{A^k}F_{\tau_{u_y}}F_{s_{u_y}}\,dz\Big]\partial_y^2 + 2\sigma_{xy_0}^k\Big[\int_{A^k}F_{\tau_{u_y}}F_{s_{u_y}}\,dz\Big]\partial_{xy}^2\Big)\\
\boldsymbol{K}_\sigma^{k\tau s}(3,3) = & \Big(\sigma_{xx_0}^k\Big[\int_{A^k}F_{\tau_{u_z}}F_{s_{u_z}}\,dz\Big]\partial_x^2 + \sigma_{yy_0}^k\Big[\int_{A^k}F_{\tau_{u_z}}F_{s_{u_z}}\,dz\Big]\partial_y^2 + 2\sigma_{xy_0}^k\Big[\int_{A^k}F_{\tau_{u_z}}F_{s_{u_z}}\,dz\Big]\partial_{xy}^2\Big)
\end{aligned}
\tag{66}
$$

The final free motion and stability equations with related boundary conditions can be written as:

Table 1
Nondimensionalized uniaxial buckling load $N_{cr} = \bar{N}_{cr}\frac{b^2}{E_{11}h^3}$ for simply supported cross-ply, MAT1.

	Nonlinear strains E_1/E_2					von Kàrmàn E_1/E_2				
	3	10	20	30	40	3	10	20	30	40
3D-[45]	5.3044	9.7621	15.0191	19.3040	22.8807	–	–	–	–	–
$LM4$[29]	5.3051	9.7628	15.0196	19.3045	22.8811	–	–	–	–	–
LD_{444}	5.3246	9.8191	15.1076	19.4138	23.0062	5.4023	9.9476	15.2813	19.6142	23.2230
LD_{424}	5.3257	9.8264	15.1321	19.4637	23.0880	5.4034	9.9551	15.3063	19.6649	23.3058
LD_{333}	5.3246	9.8191	15.1076	19.4139	23.0063	5.4023	9.9476	15.2813	19.6143	23.2230
LD_{323}	5.3257	9.8264	15.1321	19.4637	23.0880	5.4034	9.9551	15.3063	19.6650	23.3058
LD_{222}	5.3261	9.8271	15.1338	19.4667	23.0926	5.4038	9.9559	15.3080	19.6680	23.3105
LD_{411}	5.3708	9.8618	15.1611	19.4884	23.1096	5.4492	9.9911	15.3358	19.6902	23.3279
LD_{141}	5.3758	9.9041	15.2812	19.6922	23.3917	5.4543	10.0344	15.4583	19.8974	23.6143
LD_{114}	5.3377	9.8816	15.2820	19.7224	23.4567	5.4159	10.0121	15.4323	19.9288	23.6807
LD_{111}	5.3800	9.9146	15.3088	19.7452	23.4764	5.4588	10.0454	15.4868	19.9516	23.7005
EDZ_{888}	5.3247	9.8194	15.1087	19.4161	23.0098	5.4023	9.9479	15.2824	19.6165	23.2266
EDZ_{767}	5.3247	9.8201	15.1119	19.4232	23.0219	5.4023	9.9486	15.2856	19.6236	23.2386
EDZ_{444}	5.3249	9.8257	15.1345	19.4701	23.0981	5.4025	9.9542	15.3082	19.6705	23.3148
EDZ_{333}	5.3250	9.8260	15.1351	19.4712	23.0997	5.4026	9.9545	15.3089	19.6717	23.3164
EDZ_{222}	5.3377	9.8819	15.2826	19.7235	23.4582	5.4160	10.0124	15.4605	19.9299	23.6823
EDZ_{811}	5.6013	10.0399	15.3047	19.6085	23.2121	5.6825	10.1708	15.4802	19.8106	23.4306
EDZ_{181}	5.6073	10.0861	15.4312	19.8207	23.5042	5.6887	10.2181	15.6092	20.0263	23.7269
EDZ_{118}	5.3377	9.8816	15.2820	19.7225	23.4567	5.4159	10.0121	15.4599	19.9288	23.6808
EDZ_{111}	5.6129	10.0975	15.4590	19.8726	23.5866	5.6946	10.2300	15.6379	20.0796	23.8110
ED_{999}	5.3250	9.8205	15.1116	19.4211	23.0170	5.4026	9.9491	15.2854	19.6216	23.2338
ED_{888}	5.3251	9.8214	15.1140	19.4251	23.0226	5.4028	9.9500	15.2878	19.6257	23.2395
ED_{878}	5.3251	9.8214	15.1140	19.4251	23.0226	5.4028	9.9500	15.2878	19.6257	23.2395
ED_{778}	5.3251	9.8214	15.1140	19.4251	23.0226	5.4028	9.9500	15.2878	19.6257	23.2395
ED_{777}	5.3251	9.8214	15.1140	19.4251	23.0226	5.4028	9.9500	15.2878	19.6257	23.2395
ED_{654}	5.3253	9.8233	15.1371	19.4382	23.0429	5.4029	9.9519	15.2945	19.6388	23.2598
ED_{564}	5.3253	9.8263	15.1365	19.4750	23.1072	5.4029	9.9549	15.3103	19.6753	23.3236
ED_{456}	5.3253	9.8236	15.1228	19.4430	23.0510	5.4030	9.9522	15.2966	19.6436	23.2679
ED_{444}	5.3253	9.8266	15.1386	19.4798	23.1153	5.4030	9.9552	15.3123	19.6801	23.3317
ED_{333}	5.3254	9.8269	15.1392	19.4808	23.1168	5.4031	9.9555	15.3130	19.6812	23.3332
ED_{822}	5.3361	9.8578	15.2146	19.6185	23.3332	5.4144	9.9881	15.3923	19.8253	23.5585
ED_{282}	5.3643	10.0148	15.6331	20.3169	24.2918	5.4436	10.1497	15.8205	20.5372	24.5331
ED_{228}	5.3752	10.0511	15.7334	20.5097	24.6014	5.4552	10.1878	15.9247	20.7364	24.8515
ED_{222}	5.3752	10.0511	15.7335	20.5098	24.6014	5.4552	10.1878	15.9248	20.7364	24.8515
ED_{911}	5.6118	10.0728	15.3892	19.7651	23.4583	5.6936	10.2051	15.5680	19.9724	23.6839
ED_{411}	5.6121	10.0748	15.3965	19.7789	23.4789	5.6938	10.2072	15.5753	19.9862	23.7045
ED_{311}	5.6121	10.0748	15.3965	19.7789	23.4789	5.6938	10.2072	15.5753	19.9862	23.7045
ED_{211}	5.6618	10.2865	15.9381	20.6927	24.7673	5.7455	10.4256	16.1310	20.9205	25.0181
ED_{191}	5.6457	10.2429	15.8276	20.4875	24.4435	5.7287	10.3800	16.0162	20.7084	24.6851
ED_{141}	5.6458	10.2468	15.8469	20.5317	24.5202	5.7288	10.3840	16.0355	20.7524	24.7613
ED_{131}	5.6458	10.2468	15.8469	20.5317	24.5202	5.7288	10.3840	16.0355	20.7524	24.7613
ED_{121}	5.6618	10.2865	15.9381	20.6927	24.7673	5.7455	10.4256	16.1310	20.9205	25.0181
ED_{119}	5.3752	10.0511	15.7334	20.5097	24.6014	5.4552	10.1878	15.9247	20.7364	24.8515
ED_{114}	5.3752	10.0511	15.7334	20.5098	24.6014	5.4552	10.1878	15.9248	20.7364	24.8515
ED_{113}	5.3752	10.0511	15.7335	20.5097	24.6014	5.4552	10.1878	15.9248	20.7364	24.8515
ED_{112}	5.3752	10.0511	15.7335	20.5097	24.6014	5.4552	10.1877	15.9248	20.7364	24.8515
ED_{111}	5.6618	10.2865	15.9381	20.6927	24.7673	5.7455	10.4256	16.1310	20.9205	25.0181

$$\begin{aligned}
\delta u^k_{\tau_{u_x}} &: K^{\tau_{u_x}s_{u_x}}_{du_xu_x} u^k_{s_{u_x}} + K^{\tau_{u_x}s_{u_y}}_{du_xu_y} u^k_{s_{u_y}} + K^{\tau_{u_x}s_{u_z}}_{du_xu_z} u^k_{s_{u_z}} = M^{\tau_{u_x}s_{u_x}}_{u_xu_x} \ddot{u}^k_{s_{u_x}} + K_{\sigma_{u_xu_x}} u^k_{s_{u_x}} \\
\delta u^k_{\tau_{u_y}} &: K^{\tau_{u_y}s_{u_x}}_{du_yu_x} u^k_{s_{u_x}} + K^{\tau_{u_y}s_{u_y}}_{du_yu_y} u^k_{s_{u_y}} + K^{\tau_{u_y}s_{u_z}}_{du_yu_z} u^k_{s_{u_z}} = M^{\tau_{u_y}s_{u_y}}_{u_yu_y} \ddot{u}^k_{s_{u_y}} + K_{\sigma_{u_yu_y}} u^k_{s_{u_y}} \\
\delta u^k_{\tau_{u_z}} &: K^{\tau_{u_z}s_{u_x}}_{du_zu_x} u^k_{s_{u_x}} + K^{\tau_{u_z}s_{u_y}}_{du_zu_y} u^k_{s_{u_y}} + K^{\tau_{u_z}s_{u_z}}_{du_zu_z} u^k_{s_{u_z}} = M^{\tau_{u_z}s_{u_z}}_{u_zu_z} \ddot{u}^k_{s_{u_z}} + K_{\sigma_{u_zu_z}} u^k_{s_{u_z}} \\
\delta u^k_{\tau_{u_x}} &: \Pi_{du_xu_x} u^k_{s_{u_x}} + \Pi_{du_xu_y} u^k_{s_{u_y}} + \Pi_{du_xu_z} u^k_{s_{u_z}} = \Pi_{du_xu_x} \bar{u}^k_{s_{u_x}} + \Pi_{du_xu_y} \bar{u}^k_{s_{u_y}} + \Pi_{du_xu_z} \bar{u}^k_{s_{u_z}} \\
\delta u^k_{\tau_{u_y}} &: \Pi_{du_yu_x} u^k_{s_{u_x}} + \Pi_{du_yu_y} u^k_{s_{u_y}} + \Pi_{du_yu_z} u^k_{s_{u_z}} = \Pi_{du_yu_x} \bar{u}^k_{s_{u_x}} + \Pi_{du_yu_y} \bar{u}^k_{s_{u_y}} + \Pi_{du_yu_z} \bar{u}^k_{s_{u_z}} \\
\delta u^k_{\tau_{u_z}} &: \Pi_{du_zu_x} u^k_{s_{u_x}} + \Pi_{du_zu_y} u^k_{s_{u_y}} + \Pi_{du_zu_z} u^k_{s_{u_z}} = \Pi_{du_zu_x} \bar{u}^k_{s_{u_x}} + \Pi_{du_zu_y} \bar{u}^k_{s_{u_y}} + \Pi_{du_zu_z} \bar{u}^k_{s_{u_z}}
\end{aligned} \tag{67}$$

It should be bear in mind that the subscript d, in the 9 invariant nuclei, indicates that the kernels are differential operators.

6. Results

A crucial point in these methodologies is the choice of the basis functions, on which, the approximate solutions, are built with a linear combinations of unknown coefficients. In the present work, trigonometric functions have been considered,

$$\begin{aligned}
\psi_{x_{mn}}(x,y) &= \sum_{m,n} \cos\left(\frac{m\pi x}{a}\right) \sin\left(\frac{n\pi y}{b}\right) \\
\psi_{y_{mn}}(x,y) &= \sum_{m,n} \sin\left(\frac{m\pi x}{a}\right) \cos\left(\frac{n\pi y}{b}\right) \\
\psi_{z_{mn}}(x,y) &= \sum_{m,n} \sin\left(\frac{m\pi x}{a}\right) \sin\left(\frac{n\pi y}{b}\right)
\end{aligned} \tag{68}$$

Using this kind of functions, the surface integrals present in the *fundamental nuclei* can be solved analitically. It is useful to observe that the trigonometric functions are of class ∞, then in this particular case it is not important that Galerkin's method required an higher differentiability order of the approximation functions, in comparison with Ritz. For the sake of conciseness, the surface integrals for Ritz method have already been listed in a previous work of the authors [21], for Galerkin method the surface integrals are different, but can be computed in the same way. The results have been obtained using the following materials:

MAT1: E_1/E_2 variable, $G_{12}/E_2 = G_{12}/E_2 = 0.6$, $G_{23}/E_2 = 0.5$, $\nu_{12} = 0.25$, [29]
MAT2: $E_1 = 60.7$ GPa, $E_2 = 24.8$ GPa, $G_{12} = 12.0$ GPa, $\nu_{12} = 0.23$, [47]
MAT3: $E_1 = 130$ GPa, $E_2 = 9$ GPa, $G_{12} = 4.8$ GPa, $\nu_{12} = 0.28$, [25]
MAT4: $E_1/E_2 = 30$, $G_{12}/E_2 = G_{12}/E_2 = 0.5$, $G_{23}/E_2 = 0.2$, $\nu_{12} = 0.30$, [43]

In particular MAT1 is a symmetric CRFP laminate [0/90/...] with an odd number of layers N_l. The total thickness of the 0° 90° layers is the same. The results will be given using the usual acronyms system used in CUF [16], adding the possibility to encompasses all the refined hierarchal plate theories. Therefore, the ESL theories are indicated as $ED_{N_{u_x}N_{u_y}N_{u_z}}$ where E means the ESL approach, D means that the Principle of Virtual Displacements has been employed and N_{u_x}, N_{u_y}, N_{u_z} are the three different expansion orders used in the displacements field. LW theories are defined as $LD_{N_{u_x}N_{u_y}N_{u_z}}$ where the only difference is the letter L which states that Layerwise approach has been used.

6.1. Buckling analysis of symmetric cross-ply laminates

6.1.1. Uniaxial compression

A validation and assessment of more than 45 different LW, ZZ and ESL theories, built using a variable kinematics approach with hierarchical capabilities, is carried out. The results in Table 1 for the nondimensionalized critical uniaxial buckling $N_{cr} = \overline{N}_{cr}\frac{b^2}{E_{22}h^3}$ are compared with the exact 3D solution provided by Noor [45], which is based on a uniform strain state assumption. The critical loads evaluated in this paper are based on a uniform stress state approach. The more advanced and refined theories

Table 2
Nondimensionalized uniaxial and biaxial buckling load $N_{cr} = \overline{N}_{cr}\frac{b^2}{E_{11}h^3}$ for simply supported cross-ply, MAT1.

	Uniaxial compression a/h					Biaxial compression a/h				
	10	20	25	50	100	10	20	25	50	100
3D-[45]	22.8807	–	–	–	–	–	–	–	–	–
LD_{444}	23.0062	31.5120	33.0280	35.3172	35.9450	11.5031	15.7560	16.5140	17.6586	17.9725
LD_{442}	23.0063	31.5120	33.0280	35.3172	35.9450	11.5032	15.7560	16.5140	17.6586	17.9725
LD_{424}	23.0880	31.5389	33.0458	35.3219	35.9462	11.5440	15.7694	16.5229	17.6609	17.9731
LD_{244}	23.0108	31.5137	33.0291	35.3175	35.9451	11.5054	15.7568	16.5146	17.6587	17.9725
LD_{222}	23.0926	31.5405	33.0470	35.3222	35.9463	11.5463	15.7703	16.5235	17.6611	17.9731
EDZ_{888}	23.0098	31.5135	33.0290	35.3175	35.9451	11.5049	15.7567	16.5145	17.6587	17.9725
EDZ_{777}	23.0098	31.5135	33.0290	35.3175	35.9451	11.5049	15.7567	16.5145	17.6587	17.9725
EDZ_{774}	23.0098	31.5135	33.0290	35.3175	35.9451	11.5049	15.7567	16.5145	17.6587	17.9725
EDZ_{747}	23.0709	31.5334	33.0422	35.3209	35.9459	11.5354	15.7667	16.5211	17.6605	17.9730
EDZ_{477}	23.0370	31.5274	33.0389	35.3203	35.9458	11.5185	15.7637	16.5194	17.6602	17.9730
EDZ_{833}	23.0946	31.5336	33.0423	35.3209	35.9464	11.5362	15.7668	16.5211	17.6605	17.9730
EDZ_{383}	23.0377	31.5276	33.0390	35.3204	35.9458	11.5195	15.7638	16.5195	17.6602	17.9729
EDZ_{338}	23.0981	31.5473	33.0521	35.3238	35.9467	11.5490	15.7737	16.5261	17.6619	17.9733
EDZ_{333}	23.0997	31.5475	33.0522	35.3238	35.9467	11.5499	15.7738	16.5261	17.6619	17.9733
ED_{999}	23.0170	31.5171	33.0316	35.3182	35.9453	11.5085	15.7585	16.5158	17.6591	17.9726
ED_{888}	23.0226	31.5201	33.0337	35.3188	35.9454	11.5113	15.7600	16.5169	17.6594	17.9727
ED_{855}	23.0357	31.5245	33.0367	35.3196	35.9456	11.5179	15.7623	16.5183	17.6598	17.9728
ED_{585}	23.0298	31.5247	33.0371	35.3199	35.9457	11.5149	15.7623	16.5185	17.6599	17.9728
ED_{558}	23.0429	31.5291	33.0400	35.3206	35.9459	11.5577	15.7645	16.5200	17.6603	17.9729
ED_{444}	23.1153	31.5531	33.0560	35.3248	35.9469	11.5577	15.7765	16.5280	17.6624	17.9735
ED_{833}	23.1014	31.5453	33.0504	35.3232	35.9465	11.5507	15.7726	16.5252	17.6616	17.9733
ED_{383}	23.0398	31.5283	33.0395	35.3205	35.9459	11.5199	15.7641	16.5198	17.6603	17.9729
ED_{338}	23.1153	31.5531	33.0560	35.3248	35.9469	11.5577	15.7765	16.5280	17.6624	17.9735
ED_{333}	23.1167	31.5532	33.0560	35.3249	35.9469	11.5584	15.7766	16.5280	17.6624	17.9735
ED_{222}	24.6014	32.2482	33.5442	35.4642	35.9830	12.3007	16.1241	16.7721	17.7321	17.9915
ED_{111}	24.7673	32.4877	33.7972	35.7374	36.2618	12.3837	16.2439	16.8986	17.8687	18.1309

such as quasi-3D LD_{444} or EDZ_{888} and ED_{999} are in good agreement with the exact solution, proving that CUF is a successful tool to generate 2D plate theories. The analysis has been executed taken into account both the full nonlinear strains and von Kàrmàn geometric nonlinearities. It can be observed that if the full nonlinearities are performed, using a LD_{444} theory the error is 0.38% whilst using the same theory and von Kàrmàn's approximation the error is 1.85%. This result shows how the full nonlinear strains contribution is extremely useful if an accurate buckling analysis is required for thick plate, whilst for thin plates the discrepancy is negligible. A further comparison between the two different approaches is given in Fig. 5, it can be noticed that both a for three layers and a nine layers laminated plate, the theories LD_{444}^{TvK} (von Kàrmàn's approximation) and LD_{444} confirm what has been already inferred from the results in Table 1, the number of layers does not affect the results prominently. Moreover by using a $LM4_{\epsilon}$ theory where the subscript ϵ states that the axial load has been imposed via to a uniform strain state, the 3-D exact solution is completely matched. Different theories with different expansion orders have been provided in order to evaluate how the accuracy increases for a given theory. In general as expected, when the orders of the different displacement components are increased the accuracy of the approximation is improved. From Table 1 can also be observed that it is more convenient to increase the order of the expansion used in the thickness direction for all the displacements rather than increasing only a component. For instance, the theories LD_{114}, LD_{141} and LD_{411} use the same degree of freedom of the theory LD_{222}, nevertheless their accuracy is lower. Moreover increasing the expansion order for a single unknown as listed for the theories from ED_{113} to ED_{119}, ED_{131} to ED_{191} and ED_{311} to ED_{911} the accuracy in the results does not change significantly. The capability to build different plate theories by using CUF becomes extremely powerful when multifield problems for multilayered structures, such as thermoelastic and piezoelectric formulations, are addressed. In Table 1 should be also noticed that varying the orthotropic ratio the refined theories do not change the accuracy with respect to the 3D exact solution. The results for the models ED_{111}, LD_{111}, EDZ_{111}, are higher than the others and in particular ED_{111}, EDZ_{111} are higher than FSDT [29]. This is a pathology that is peculiar of the linear models which retain the full 3-D constitutive law, and that has been referred to in [18], as *Poisson Locking* or *Thickness Locking*.

6.1.2. Uniaxial and biaxial compression

In the following parts the results will be obtained referring to the full nonlinear strains. In Table 2 nondimensionalized critical load for uniaxial and biaxial compression are shown. A further extensive assessment is carried out in order to highlight the accuracy of the proposed hierarchic modeling technique for the two different load configurations. Varying the thickness ratio all the presented formulations consistently converge toward CLPT results when the plate becomes thinner. This phenomenon can be also observed in Fig. 4 for biaxial compression tacking into consideration two different orthotropic ratio. As already observed for the uniaxial compression, also for the biaxial compression in Table 2, ED_{111} model is affected by Poisson locking. When the biaxial compression is considered then critical loads are halved in comparison with the critical loads evaluated for uniaxial compression.

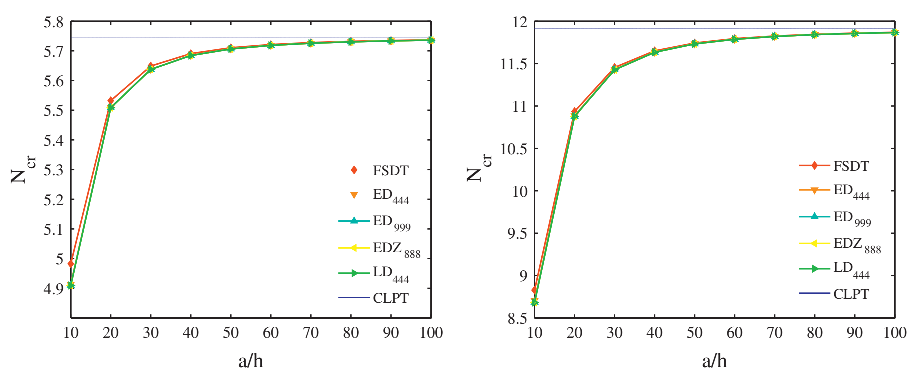

(a) $E_1/E_2 = 10$ (b) $E_1/E_2 = 25$

Fig. 4. Nondimensionalized biaxial buckling load $N_{cr} = \overline{N}_{cr}\frac{b^2}{E_{11}h^3}$, varying the thickness ratio a/h, MAT1.

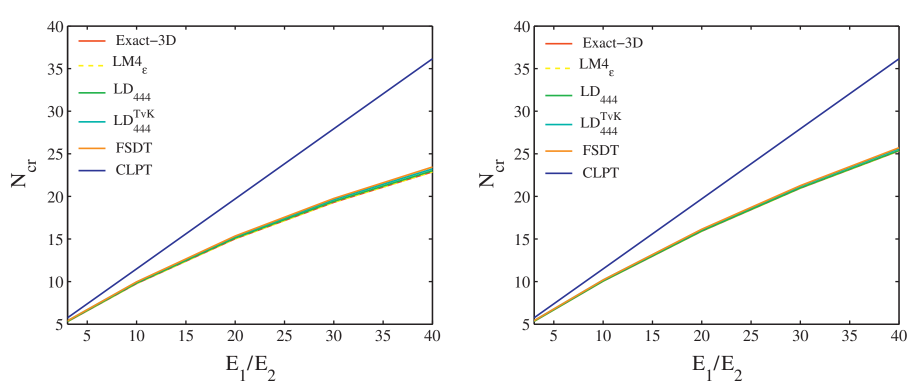

(a) $N_l = 3$ (b) $N_l = 9$

Fig. 5. Nondimensionalized uniaxial buckling load $N_{cr} = \overline{N}_{cr}\frac{b^2}{E_{11}h^3}$, varying the orthotropic ratio, MAT1.

6.2. Buckling analysis of symmetric angle-ply laminates

A convergence analysis of the uniaxial critical load in Fig. 6, by using CLPT, is carried out. The number of the half-waves is increased until m, $n = 18$. The critical load is evaluated varying the lamination angle and considering two different lamination schemes $[\theta]$ and $[\theta/-\theta/\theta]$. Between the two cases the rate of convergence does not change significantly. On the contrary the nondimensionalized critical load undergoes to a consistent variation, increasing in the $[\theta/-\theta/\theta]$ configuration. In both cases a sharp decrease is visible after the lamination angle $\theta = 55°$, whereas the maximum nondimensionalized critical load is reached for $\theta = 0°$ in the first lamination scheme and for $\theta = 45°$ in the second one. Fig. 7 shows, once the convergence is reached, what is the influence of the different theories varying the thickness ratio a/h. As expected for thin plate CLPT, FSDT and the refined ED_{444} theory, are totally agree, instead for thick plate, when the 3D effects become more pronounced the ED_{444} theory shows the best behavior. In Table 3 the two stacking sequence of the layout are [0°/90°/0°] and [0°/75°/90°/75°/0°]. Ritz (RM) and Galerkin (GM) approximation methods are carried out, the results for Ritz method are compared with FEM [43]. The discrepancy between the two methodologies is higher for the lamination scheme [0°/90°/0°], when nondimensionalized uniaxial load is evaluated, however it does not exceed the 4.10% reached with the FSDT. As can be observed in Table 4 the discrepancy range increases when the pure shear

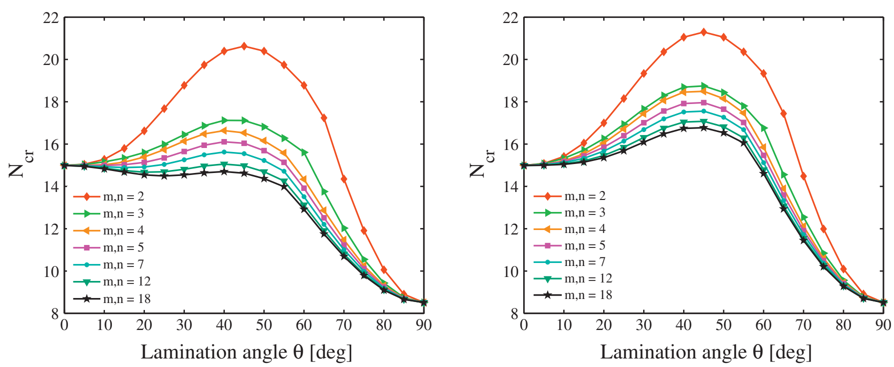

(a) Lamination scheme: $[\theta]$ (b) Lamination scheme: $[\theta/-\theta/\theta]$

Fig. 6. Convergence study for regular symmetric angle-ply under uniaxial compression, with lamination angle ranging from 0° to 90°, MAT3.

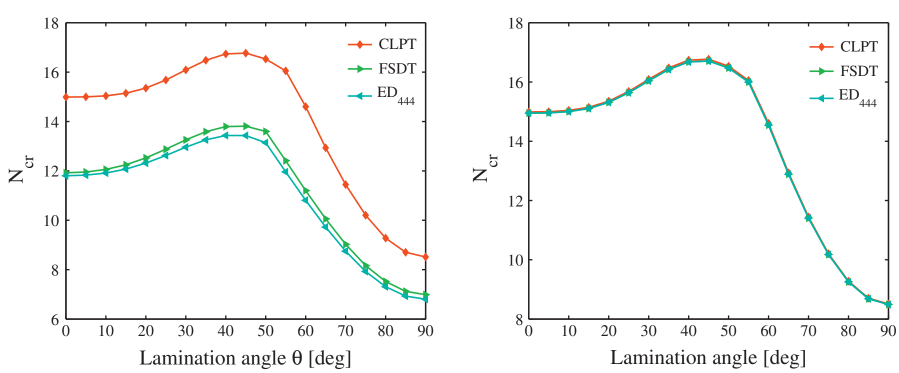

(a) $a/h = 10$ (b) $a/h = 100$

Fig. 7. Nondimensionalized uniaxial buckling load $N_{cr} = \overline{N}_{cr}\frac{b^2}{E_{11}h^3}$, varying the refined theories, MAT3.

Table 3
Uniaxial buckling load $N_{y_{cr}}10^{-4}$ N/ m for simply supported square plate, with different lamination schemes, MAT4.

	[0°/90°/0°]			Diff% RM-FEM	[0°/75°/90°/75°/0°]			Diff% RM-FEM
	RM	GM	FEM [43]		RM	GM	FEM [43]	
LD_{222}	1.5340	1.5340	1.589	3.59	2.8858	2.6152	2.926	2.64
EDZ_{222}	1.5387	1.5387	–	–	2.9377	2.7006	–	–
ED_{444}	1.5450	1.5450	–	–	2.8953	2.8639	–	–
ED_{333}	1.5450	1.5450	–	–	2.8953	2.8639	–	–
ED_{222}	1.5727	1.5727	–	–	2.9765	2.9659	–	–
ED_{711}	1.6287	1.6287	–	–	2.9394	2.8473	–	–
ED_{171}	1.5727	1.5727	–	–	3.0156	2.9469	–	–
ED_{117}	1.5727	1.5727	–	–	2.9764	2.9659	–	–
ED_{111}	1.6331	1.6331	–	–	3.0218	3.0106	–	–
FSDT	1.5639	1.5639	1.628	4.10	2.9768	3.0105	3.028	1.72

Table 4
Nondimensionalized pure shear buckling load $N_{xy_{cr}} 10^{-4}$ N/m for simply supported square plate, with different lamination schemes, MAT4.

	[0°/90°/0°]			Diff% RM-FEM	[0°/75°/90°/75°/0°]			Diff% RM-FEM
	RM	GM	FEM [43]		RM	GM	FEM [43]	
LD_{222}	4.5986	4.5986	5.223	13.58	4.9752	5.2914	7.071	42.12
EDZ_{222}	4.6411	4.6411	–	–	5.1770	5.4706	–	–
ED_{444}	4.7071	4.7071	–	–	5.0249	5.4488	–	–
ED_{333}	4.7072	4.7072	–	–	5.0251	5.4490	–	–
ED_{222}	4.9879	4.9879	–	–	5.3933	5.8598	–	–
ED_{711}	4.7696	4.7696	–	–	5.1119	5.5211	–	–
ED_{171}	5.1129	5.1129	–	–	5.4541	5.8809	–	–
ED_{117}	4.9879	4.9879	–	–	5.3933	5.8598	–	–
ED_{111}	5.1305	5.1305	–	–	5.4820	5.9497	–	–
FSDT	4.9881	4.9881	5.669	13.65	5.3951	5.8617	7.719	43.07

Table 5
Nondimensionalized fundamental frequency parameter $\hat{\omega} = \omega\sqrt{\frac{a^4\rho}{E_2 h^2}}$, varying the refined theories, of simply supported square plates, with regular symmetric angle-ply lamination scheme, MAT2.

	m, n	[15°/−15°/15°]			[30°/−30°/30°]			[45°/−45°/45°]		
		RM	GM	GGM	RM	GM	GGM	RM	GM	GGM
FSDT	2	4.3414	4.3497	4.3420	4.4904	4.5115	4.4910	4.5652	4.5910	4.5652
	4	4.3355	4.3474	4.3370	4.4737	4.5040	4.4763	4.5439	4.5809	4.5460
	6	4.3330	4.3467	4.3349	4.4666	4.5018	4.4706	4.5347	4.5777	4.5385
	8	4.3316	4.3464	4.3338	4.4627	4.5007	4.4674	4.5296	4.5763	4.5345
	10	4.3307	4.3463	4.3330	4.4601	4.5002	4.4654	4.5263	4.5755	4.5319
	12	4.3301	4.3462	4.3325	4.4584	4.4999	4.4639	4.5240	4.5750	4.5301
ED_{222}	2	4.3634	4.3718	4.3638	4.5141	4.5357	4.5144	4.5897	4.6164	4.5895
	4	4.3573	4.3696	4.3587	4.4972	4.5283	4.4994	4.5680	4.6062	4.5698
	6	4.3549	4.3689	4.3567	4.4900	4.5260	4.4936	4.5587	4.6030	4.5623
	8	4.3535	4.3686	4.3555	4.4859	4.5251	4.4904	4.5535	4.6016	4.5582
	10	4.3526	4.3685	4.3548	4.4834	4.5245	4.4884	4.5502	4.6009	4.5556
	12	4.3519	4.3684	4.3542	4.4816	4.5242	4.4869	4.5479	4.6004	4.5538
ED_{444}	2	4.3451	4.3535	4.3456	4.4942	4.5156	4.4946	4.5690	4.5953	4.5687
	4	4.3391	4.3512	4.3405	4.4774	4.5083	4.4797	4.5476	4.5853	4.5493
	6	4.3366	4.3506	4.3384	4.4703	4.5061	4.4739	4.5384	4.5822	4.5418
	8	4.3352	4.3503	4.3373	4.4663	4.5051	4.4707	4.5332	4.5808	4.5378
	10	4.3343	4.3501	4.3365	4.4638	4.5046	4.4687	4.5299	4.5800	4.5352
	12	4.3337	4.3501	4.3360	4.4620	4.5042	4.4672	4.5276	4.5796	4.5334
EDZ_{222}	2	4.3543	4.3628	4.3548	4.5041	4.5257	4.5044	4.5793	4.6058	4.5790
	4	4.3483	4.3605	4.3496	4.4872	4.5183	4.4894	4.5576	4.5957	4.5594
	6	4.3458	4.3598	4.3475	4.4800	4.5160	4.4836	4.5483	4.5925	4.5518
	8	4.3444	4.3595	4.3464	4.4760	4.5150	4.4805	4.5431	4.5911	4.5478
	10	4.3435	4.3594	4.3457	4.4734	4.5145	4.4784	4.5397	4.5903	4.5452
	12	4.3428	4.3593	4.3451	4.4716	4.5142	4.4769	4.5374	4.5899	4.5434
EDZ_{444}	2	4.3451	4.3535	4.3456	4.4941	4.5156	4.4945	4.5689	4.5953	4.5687
	4	4.3391	4.3512	4.3404	4.4773	4.5082	4.4796	4.5474	4.5852	4.5492
	6	4.3365	4.3505	4.3384	4.4701	4.5060	4.4737	4.5380	4.5820	4.5416
	8	4.3351	4.3503	4.3372	4.4661	4.5050	4.4705	4.5330	4.5807	4.5375
	10	4.3342	4.3501	4.3364	4.4635	4.5045	4.4685	4.5296	4.5799	4.5349
	12	4.3336	4.3500	4.3359	4.4617	4.5041	4.4670	4.5273	4.5794	4.5330

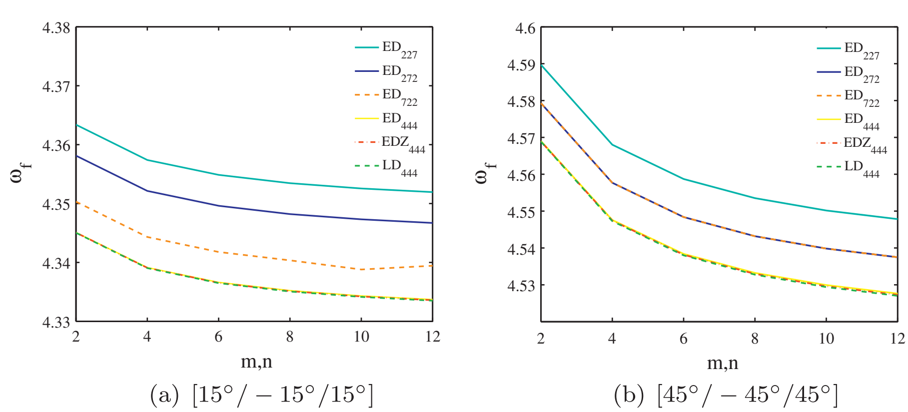

Fig. 8. Convergence study for simply supported regular symmetric angle ply, varying the number of half-waves, MAT2.

Table 6
Nondimensionalized fundamental frequency parameter $\hat{\omega} = \omega\sqrt{\frac{a^4\rho}{E_2h^2}}$, varying the thickness ratio, of simply supported square plates, with regular symmetric angle-ply lamination scheme for an ED_{222} model, MAT2.

a/h	m, n	[15°/−15°/15°]			[30°/−30°/30°]			[45°/−45°/45°]		
		RM	GM	GGM	RM	GM	GGM	RM	GM	GGM
10	2	4.3634	4.3718	4.3638	4.5141	4.5357	4.5144	4.5897	4.6164	4.5895
	4	4.3574	4.3696	4.3587	4.4972	4.5283	4.4994	4.5680	4.6062	4.5698
	6	4.3549	4.3689	4.3567	4.4900	4.5260	4.4936	4.5587	4.6030	4.5623
	8	4.3535	4.3686	4.3555	4.4859	4.5251	4.4904	4.5535	4.6016	4.5582
	10	4.3526	4.3685	4.3548	4.4834	4.5245	4.4884	4.5501	4.6009	4.5556
	12	4.3519	4.3684	4.3542	4.4816	4.5242	4.4869	4.5479	4.6004	4.5538
20	2	4.4745	4.4832	4.4746	4.6325	4.6553	4.6324	4.7118	4.7404	4.7116
	4	4.4684	4.4808	4.4693	4.6147	4.6473	4.6168	4.6887	4.7293	4.6909
	6	4.4658	4.4801	4.4674	4.6072	4.6449	4.6110	4.6788	4.7259	4.6833
	8	4.4644	4.4798	4.4664	4.6030	4.6438	4.6081	4.6733	4.7244	4.6794
	10	4.4635	4.4797	4.4658	4.6003	4.6433	4.6063	4.6698	4.7235	4.6771
	12	4.4629	4.4796	4.4654	4.5985	4.6429	4.6050	4.6673	4.7230	4.6754
25	2	4.4886	4.4973	4.4886	4.6475	4.6704	4.6474	4.7273	4.7561	4.6754
	4	4.4824	4.4948	4.4833	4.6296	4.6624	4.6316	4.7040	4.7450	4.7063
	6	4.4799	4.4942	4.4814	4.6221	4.6599	4.6259	4.6940	4.7415	4.6987
	8	4.4784	4.4939	4.4805	4.6179	4.6589	4.6230	4.6885	4.7399	4.6948
	10	4.4775	4.4937	4.4799	4.6152	4.6583	4.6213	4.6849	4.7391	4.6925
	12	4.4769	4.4936	4.4795	4.6133	4.6580	4.6201	4.6824	4.7385	4.6910
50	2	4.5076	4.5163	4.5075	4.6678	4.6909	4.6676	4.7482	4.7773	4.7479
	4	4.5014	4.5138	4.5022	4.6498	4.6828	4.6517	4.7247	4.7661	4.7270
	6	4.4988	4.5132	4.5003	4.6421	4.6803	4.6461	4.7146	4.7625	4.7194
	8	4.4974	4.5129	4.4994	4.6379	4.6792	4.6433	4.7090	4.7609	4.7157
	10	4.4965	4.5127	4.4989	4.6352	4.6786	4.6416	4.7054	4.7601	4.7135
	12	4.4959	4.5126	4.4986	4.6333	4.6783	4.6406	4.7029	4.7595	4.7120
100	2	4.5123	4.5211	4.5123	4.6729	4.6961	4.6727	4.7535	4.7827	4.7532
	4	4.5062	4.5186	4.5070	4.6548	4.6879	4.6568	4.7299	4.7714	4.7323
	6	4.5036	4.5180	4.5051	4.6472	4.6854	4.6511	4.7198	4.7678	4.7247
	8	4.5022	4.5177	4.5042	4.6430	4.6843	4.6484	4.7142	4.7662	4.7210
	10	4.5013	4.5175	4.5037	4.6403	4.6837	4.6468	4.7106	4.7654	4.7188
	12	4.5007	4.5174	4.5034	4.6384	4.6834	4.6458	4.7081	4.7648	4.7174

Table 7
First 6 nondimensionalized frequency parameters $\hat{\omega} = \omega\sqrt{\frac{a^4\rho}{E_2h^2}}$ of simply supported square plate, with lamination scheme [30°/−30°/30°], MAT2.

	a/h		$\hat{\omega}_1$	$\hat{\omega}_2$	$\hat{\omega}_3$	$\hat{\omega}_4$	$\hat{\omega}_5$	$\hat{\omega}_6$
Ritz (algebric polynomial)[47]		CLPT	4.631	10.45	12.44	17.91	21.17	25.37
Ritz	10	CLPT	4.6021	10.2558	12.1876	17.3474	20.1317	20.5634
		FSDT	4.4813	9.7527	11.3719	15.9570	18.3487	20.5634
		ED_{444}	4.4620	9.6769	11.2497	15.7530	18.1054	20.5611
		EDZ_{444}	4.4617	9.6763	11.2490	15.7513	18.1046	20.5611
	100	CLPT	4.6396	10.4649	12.4342	17.9279	20.9231	25.0090
		FSDT	4.6383	10.4577	12.4251	17.9092	20.8980	24.9685
		ED_{444}	4.6382	10.4568	12.4235	17.9064	20.8942	24.9618
		EDZ_{444}	4.6382	10.4568	12.4235	17.9064	20.8942	24.9617
Galerkin	10	CLPT	4.6461	10.0267	12.3921	17.0181	20.2304	20.5648
		FSDT	4.5233	9.5552	11.5422	15.7264	18.4051	20.5648
		ED_{444}	4.5042	9.4821	11.4175	15.5337	18.1573	20.5625
		EDZ_{444}	4.5041	9.4816	11.4169	15.5322	18.1562	20.5625
	100	CLPT	4.6819	10.2287	12.6445	17.5948	21.0236	25.0924
		FSDT	4.6826	10.2241	12.6334	17.5756	20.9979	25.0514
		ED_{444}	4.6832	10.2221	12.6339	17.5717	20.9957	25.0451
		EDZ_{444}	4.6832	10.2221	12.6339	17.5717	20.9957	25.0451
Generalized Galerkin	10	CLPT	4.6098	10.2622	12.1711	17.3284	20.1291	20.5537
		FSDT	4.4871	9.7490	11.3431	15.9345	18.3285	20.5537
		ED_{444}	4.4672	9.6730	11.2188	15.7318	18.0832	20.5387
		EDZ_{444}	4.4670	9.6724	11.2180	15.7301	18.0822	20.5386
	100	CLPT	4.6462	10.4674	12.4191	17.9088	20.9202	24.9646
		FSDT	4.6461	10.4640	12.4082	17.8899	20.8952	24.9228
		ED_{444}	4.6455	10.4640	12.4049	17.8887	20.8900	24.9146
		EDZ_{444}	4.6455	10.4640	12.4049	17.8887	20.8900	24.9146

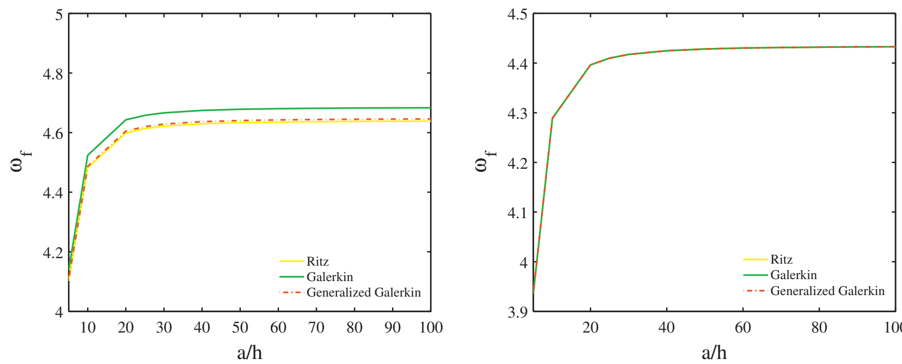

(a) [30°/ − 30°/30°] (b) [0°/ − 0°/0°]

Fig. 9. Influence of the boundary terms for a regular symmetric angle-ply, varying the thickness ratio, MAT2.

buckling load $N_{xy_{cr}}$ is computed, indeed for this case the maximum difference is obtained with the layout [0°/75°/90°/75°/0°] reaching 43.07%.

6.3. Vibration analysis of symmetric angle-ply laminates

This section deals with the vibration analysis of anisotropic plates. Different stacking sequence of the layout are presented, and different methodologies such as Ritz (RM), Galerkin (GM) and Generalized Galerkin (GGM) are performed. GGM has highlighted that the boundary terms are extremely important when, depending on the lamination schemes or the shape functions, they are not zero. Understandably, when GGM is applied for anisotropic plates, taking into account the boundary terms the discrepancy range in comparison with RM is low. Moreover, such difference grows up, increasing the lamination angle. In Table 5 a convergence analysis is carried out in order to show the influence of the variable-kinematics upon the rate of convergence. Results are shown for some increasing values of half-waves m, n. Note that a square selection strategy is adopted, i.e., the same number of Ritz terms is used in the expansion along x and y directions. As expected, all the frequency parameters monotonically decrease with the increase in the number of admissible functions, approaching the exact values. From the tabulated results, it is found that the rate of convergence is not affected by the assumed plate theory. This can also be observed in Fig. 8 where different high order and layerwise theories are shown, for two different lamination schemes. In Table 6 the convergence analysis is evaluated varying the thickness ratio. It can be observed that the rate of convergence is not affected prominently for the first frequency parameter. Nevertheless as shown in [30], it influences significantly higher frequencies and convergence is faster when the thickness dimension becomes significant. On the contrary the lamination schemes have a strong influence, indeed for a lower lamination angle the convergence is faster, as visible in Fig. 8. In Table 7 the first six frequencies are evaluated for a lamination scheme of [30°/−30°/30°], the results are compared with those obtained by Qatu in [47] for thin plate (CLPT) and employing a Ritz formulation by using algebraic polynomials (64 DOF). In the present analysis the nondimensionalized frequency parameters are evaluated with m, $n = 12$. This number of half-waves has been chosen because represents the best trade off between accuracy and computational time. As proved previously and also in other papers [21] for anisotropic plate, and [16,29,27] for orthotropic plate, CLPT can be used with good accuracy for thin plate, whilst for thick plate more advanced hierarchic models such as ESL, ZZ, and LW should be used in order to obtain the desirable accuracy. Finally, in Fig. 9 the convergence of the nondimentionalized frequency parameter $\hat{\omega} = \omega\sqrt{\frac{a^4\rho}{E_2h^2}}$ varying the thickness ratio is shown and the effect of the boundary terms is investigated for two different lamination schemes, by using a LD_{444} theory. For a lamination scheme [30°/−30°/30°] the boundary terms are not zero, and the application of the GGM stabilizes the results in respect to RM. If a lamination scheme [0°/−0°/0°] is considered then the boundary terms are zero and the three different methodologies lead to the same results.

7. Conclusions

The accuracy of advanced and refined plate theories built with a hierarchical approach, for buckling and vibration analysis has been investigated. Buckling analysis has been carried out taking into account uniaxial, biaxial and pure shear loads of cross-ply and regular symmetric angle ply. von Kàrmàn's approximation and exact nonlinear strain–displacement relations have been accounted for, along with preloads corresponding to a constant stress state. An extensive assessment of ESL, ZZ, and LW theories has been provided to establish the accuracy of each theory. Vibration analysis of regular angle-ply has also been investigated. Convergence analysis varying theory and thickness ratio has been computed. All the results have been obtained referring to approximation methods such as Ritz, Galerkin and Generalized Galerkin embedded in the framework of CUF. The influence of the boundary terms has been discussed. From the analysis the following main conclusion can be drawn:

- Refined plate theories show their accuracy when a 3D effects appear for thick plate analysis, and reduce to CLPT when thin plate are addressed, both for buckling and vibration analysis.
- The use of the exact nonlinear strain–displacement relations gives an higher accuracy than von Kàrmàn's approximation when an accurate bucking analysis is required for thick plate.
- When many terms are considered in the approximation methods the accuracy of the results for the regular symmetric angle ply, or for the cross-ply with in plane shear load, is higher than the FEM.
- When building the advanced plate theories is more convenient to increase the order of the expansion used in the thickness direction for all the displacements rather than increasing only a component.
- The introduction of the boundary terms in the analysis, performing Generalized Galerkin, becomes extremely useful when such terms are not zero, which happens when computing angle-ply lamination schemes. When the boundary terms are zero then the three methodologies Ritz, Galerkin and Generalized Galerkin lead to the same results.

- The convergence is fast both for bucking and vibration analysis, due to the trigonometric basis functions that satisfy both the mechanical and the geometrical boundary conditions. Theories and thickness ratio do not affect it, when fundamental frequency parameter is evaluated.

References

[1] Ambartsumian S. Theory of anisotropic plates. Fizmargiz, Moskva Technomic, Stanford; 1970.
[2] Ashton J, Whitney J. Theory of laminated plates. Technomic Publishing; 1970.
[3] Bushnell D. Computerized buckling analysis of shells. Dordrecht, The Netherlands: M. Nihhoff; 1985.
[4] Carrera E. A class of two-dimensional theories for anisotropic multilayered plates analysis: Atti accademia delle scienze Torino. Mem Sci Fis 1995:49–87.
[5] Carrera E. C_0^z requirements-models for the two dimensional analysis of multilayered structures. Compos Struct 1997;37:373–84.
[6] Carrera E. Evaluation of layer-wise mixed theories for laminated plate analysis. AIAA J 1998;26:830–9.
[7] Carrera E. Mixed layer-wise models for multilayer plate analysis. Compos Struct 1998;43:57–70.
[8] Carrera E. A refined multilayered finite element model applied to linear and nonlinear analysis of sandwich plate. Compos Sci Technol 1998;58:1553–69.
[9] Carrera E. A study of transverse normal stress effects on vibration of multilayered plates and shells. J Sound Vib 1999;225:803–29.
[10] Carrera E. Transverse normal stress effects in multilayered plates. ASME J Appl Mech 1999;66:1004–12.
[11] Carrera E. A priori vs a posteriori evaluation of transverse stresses in multilayered orthotropic plates. Compos Struct 2000;48:245–60.
[12] Carrera E. Single-layer vs multi-layers plate modeling on the basis of reissner's mixed theorem. AIAA J 2000;38:342–3.
[13] Carrera E. Developments, ideas, and evaluation based upon reissner's mixed variational theorem in the modeling of multilayered plates and shells. Appl Mech Rev 2001;54:301–29.
[14] Carrera E. Theories and finite elements for multilayered anisotropic composite plates and shells. Arch Comput Methods Eng 2002;9(2):87–140.
[15] Carrera E. Historical review of zig-zag theories for multilayered plates and shells. Appl Mech Rev 2003;56:287–308.
[16] Carrera E. Theories and finite elements for multilayered plates and shells: a unified compact formulation with numerical assessment and benchmarking. Arch Comput Methods Eng 2003;10(3):216–96.
[17] Carrera E. On the use of Murakami's zig zag function in the modeling of layered plates and shells. Compos Struct 2004;82:541–54.
[18] Carrera E, Brischetto S. Analysis of thickness locking in classical, refined and mixed multilayered plate theories. Compos Struct 2008;82(4):549–62.
[19] Carrera E, Demasi L. Classical and advanced multilayered plate elements based upon pvd and rmvt. Part 1: derivation of finite element matrices. Int J Numer Methods Eng 2002;55:191–231.
[20] Carrera E, Demasi L. Classical and advanced multilayered plate elements based upon pvd and rmvt. Part 2: numerical implementation. Int J Numer Methods Eng 2002;55:253–91.
[21] Carrera E, Fazzolari F, Demasi L. Vibration analysis of anisotropic simply supported plates by using variable kinematic and Rayleigh-Ritz method. J Vib Acoust 2011.
[22] Carrera E, Miglioretti F, Petrolo M. Accuracy of refined finite elements for laminated plate analysis. Compos Struct 2011;97:1311–27.
[23] Carrera E, Petrolo M. Guidelines and recommendations to construct theories for metallic and composite plates. AIAA J 2010;48:2852–66.
[24] Carrera E, Petrolo M. On the effectiveness of higher-order terms in refined beam theories. J Appl Mech 2011;78:021013-1–021013-17.
[25] Darvizeh M, Darvizeh A, Ansari R, Sharma C. Buckling analysis of generally laminated composite plates (generalized differential quadrature rules versus RayleighRitz method). Compos Struct 2004;63:69–74.
[26] Demasi L. Refined multilayered plate elements based on Murakami zig-zag functions. Compos Struct 2005;70:308–16.
[27] Demasi L. ∞^3 hierarchy plate theories for thick and thin composite plate: the generalized unified formulation. Compos Struct 2008;85:256–70.
[28] Demasi L. ∞^6 plate theories based on generalized unified formulation. Part ii: layerwise theories. Compos Struct 2008;85:256–70.
[29] D'Ottavio M, Carrera E. Variable-kinematics approach for linearized buckling analysis of laminated plates and shells. AIAA J 2010;48(9):256–70.
[30] Dozio L, Carrera E. A variable kinematic Ritz formulation for vibration study of quadrilateral plates with arbitrary thickness. J Sound Vib 2011;330:4611–32.
[31] Ferreira A, Roque C, Carrera E, Cinefra M. Analysis of thick isotropic and cross-ply laminated plates by radial basis functions and a unified formulation. J Sound Vib 2011;330(4):771.
[32] Germain S. Researches sur la theorie des surfaces elastiques, Paris; 1821.
[33] Hearmon R. The fundamental frequency of vibration of rectangular wood and ply-wood plates. Proc Phys Soc (London) 1946;58:7892.
[34] Jones RM. Mechanics of composite materials. 2nd ed. United States: TAYLOR & FRANCIS; 1998.
[35] Lagrange JL. Note communiquee aux commissaires pour le prix de la surface elastique, Paris; 1811.
[36] Leissa A. Condition for laminated plates to remain flat under inplane loading. Compos Struct 1986;6:261–70.
[37] Leissa A, Narita Y. Vibration studies for simply supported symmetrically laminated rectangular plates. Compos Struct 1989;12:113–32.
[38] Lekhnitski S. Strength calculation of composite beams. Vestnik inzhen i tekhnikov N 9; 1935.
[39] Lekhnitski S. Anisotropic plates. Moscow: GITTL; 1957.
[40] Mindlin R. Influence of rotary inertia and shear on flexural motions of isotropic elastic plates. J Appl Mech 1951;18(10):31–8.
[41] Mohan D, Kingsbury H. Free vibrations of generally laminated orthotropic plates. J Acoust Soc Am Technomic Stanford 1970(50):266–9.
[42] Murakami H. Laminated composite plate theory with improved in-plane response. J Appl Mech Technomic Stanford 1986(53):601–66.
[43] Nali P, Carrera E, Lecca S. Assessments of refined theories for buckling analysis of laminated plates. Compos Struct 2011;93:456–64.
[44] Noor A. Free vibration of multilayered composite plates. AIAA J 1973;11:1038–9.
[45] Noor A. Stability of multilayered composite plates. Fiber Sci Technol 1975;8:81–9.
[46] Qatu M. Free vibration of laminated composite rectangular plates. Int J Solids Struct 1991;28:941–54.
[47] Qatu M. Vibration of laminated shells and plates. 1st ed. Elsevier; 2004.
[48] Reddy JN. Mechanics of laminated composite plates and shells. Theory and analysis. CRC Press; 2004.
[49] Reissner E. The effect of transverse shear deformation on the bending of elastic plates. J Appl Mech 1945;67:A67–77.
[50] Reissner E. On a certain mixed variational theorem and a proposed application. Int J Numer Methods Eng 1984;20(7):1366–8.
[51] Reissner E, Stavsky Y. Bending and stretching of certain types of heterogeneous anisotropic elastic plates. J Appl Mech 1961;28(3):402–8.
[52] Ren J. Bending theory of laminated plates. Compos Sci Technol 1986;27:225–48.
[53] Ren J. A new theory of laminated plates. Compos Sci Technol 1986;26:225–39.
[54] Riks E. Buckling. In: Stein E, de Borst R, Hughes TJR, editors. Encyclopedia of computational mechanics, vol. 2. New York: Wiley; 2004.
[55] Smith C. Some new types of orthotropic plates laminated of orthotropic materials. J Appl Mech 1953;20:286–8.
[56] Soedel W. Vibrations of shells and plates. 2nd ed. New York: Marcel Dekker; 2004.
[57] Timoshenko SP. Theory of elastic stability. New York: McGraw Hill; 1961.
[58] Timoshenko SP. History of strength of materials. New York: Dover Publication; 1983.
[59] Tsai SW. Composites design. 4th ed. Think Composites: Dayton; 1988.
[60] Vinson J, Sierakowski R. The behaviour of structures composed of composite materials. Dordrecht, The Netherlands: Martinus Nijhoff Publishers; 1986.
[61] Whitney J. The effects of transverse shear deformation on the bending of laminated plates. J Compos Mater 1969;3:534–47.
[62] Whitney J. Structural analysis of laminated anisotropic plates. Technomic Publishing; 1987.
[63] Yu W. A new theory of elastic sandwich plates one dimensional case. ASME J Appl Mech 1959;37:1031–6.